Occurrence of tumors in descendants of CBA male mice prenatally treated with diethylstilbestrol. Int J Cancer. 1992; 50: 131–5.
36 Waker BE, Haven MI. Intensity of multigenerational carcinogenesis from diethylstilbestrol in mice. Carcinogenesis. 1997; 18: 791–3.
37 Nagao T. Multigeneration effects of endocrine disrupting chemicals with special reference to teratogenesis by paternal exposure to synthetic hormones. Environ Mutagen Res. 1999; 21: 267–72.
38 Cunningham A, Klopman G, Rosenkranz HS. The carcinogenicity of diethylstilbestrol: structural evidence for a non-genotoxic mechanism. Arch Toxicol. 1996; 70: 356–61.
39 Williams GM. Methods for evaluating chemical genotoxicity. Annu Rev Pharmacol Toxicol. 1989; 29: 189–211.
40 Cohen SM, Ellwein LB. Cell proliferation in carcinogenesis. Science. 1990; 249: 1007–11.
41 Kunkel TA. DNA replication fidelity. J Biol Chem. 1992; 267: 18251–4.
42 Watson RE, Goodman JI. Epigenetics and DNA methylation come of age in toxicology. Toxicol Sci. 2002; 67: 11–6.
43 Feinberg AP. Cancer epigenetics takes center stage. Proc Natl Acad Sci USA. 2001; 98: 392–4.
44 Klaunig JE, Kamendulis LM, Xu Y. Epigenetic mechanisms of chemical carcinogenesis. Hum Exp Toxicol. 2000; 19: 543–55.
45 Riddihough G, Pennisi E. The evolution of epigenetics. Science. 2001; 293: 1063.
46 Trosko E, Chang CC, Madhukar BV, Oh SY. Modulators of gap junction function: The scientific basis of epigenetic toxicology. *In Vitro* Toxicol. 1990; 3: 9–26.
47 Holliday R. Inheritance of epigenetic defects. Science. 1987; 238: 163–70.
48 Lord BI, Woolford LB, Wang L, Stones VA, McDonald D, Lorimore SA, Papworth D, Wright EG, Scott D. Tumour induction by methyl-nitroso-urea following preconceptional paternal contamination with plutonium-239. Brit J Cancer. 1998; 78: 301–11.
49 Jablonka E, Lamb M. Epigenetic inheritance and evolution. Oxford: Oxford University Press; 1995.
50 Li S, Washburn KA, Moore R, Uno T, Teng C, Newbold RR, McLachlan JA, Negishi M. Developmental exposure to diethylstilbestrol elicits demethylation of estrogen-responsive lactoferrin gene in mouse uterus. Cancer Res. 1997; 57: 4356–9.
51 Li S, Hansman R, Newbold R, Davis B, McLachlan JA, Barrett JC. Neonatal diethylstilbestrol exposure induced persistent elevation of c-fos expression and hypomethylation in its exon-4 in mouse uterus. Mol Carcinog. 2003; 38: 78–84.
52 Holliday R. DNA methylation and epigenetic inheritance. Philos Trans R Soc Lond B Biol Sci. 1990; 326: 329–38.
53 Anway MD, Cupp AS, Uzumen M, Skinner MK. Epigenetic transgenerational actions of endocrine disruptors and male fertility. Science. 2005; 308: 1466–9.
54 Kaiser J. Endocrine disrupters trigger fertility problems in multiple generations. Science. 2005; 308: 1391–2.
55 Crews D, Gore AC, Hsu TS, Dangleben NL, Spinetta M, Schallert T, Anway MD, Skinner MK. Transgenerational epigenetic imprints on male preference. Proc Natl Acad Sci USA. 2007; 104: 5942–6.
56 Dolinoy DC, Huang D, Jirtle RL. Maternal nutrient supplementation counteracts bisphenol A-induced DNA hypomethylation in early development. Proc. Natl Acad Sci USA. 2007; 104: 13056–61.
57 Titus-Ernstoff L, Troisi R, Hatch EE, Wise LA, Palmer J, Hyer M, Kaufman R, Adam E, Strohsnitter W, Noller K, Herbst AL, Gibson-Chambers J, Hartge P, Hoover RN. Menstrual and reproductive characteristics of women whose mothers were exposed in utero to diethylstilbestrol (DES). Int J Epidemiol. 2006; 35: 862–8.
58 Waker BE. Uterine tumors in old female mice exposed prenatally to diethylstilbestrol. J Natl Cancer Inst. 1983; 70: 177–81.
59 Newbold RR, McLachlan JA. Vaginal adenosis and adenocarcinoma in mice exposed prenatally or neonatally to diethylstilbestrol. Cancer Res. 1982; 42: 2003–11.
60 McLachlan JA, Newbold RR, Bullock BC. Long-term effects on the female mouse genital tract associated with prenatal exposure to diethylstilbestrol. Cancer Res. 1980; 40: 3988–99.
61 McLachlan JA, Newbold RR, Shah HC, Hogan M, Doxon RL. Reduced fertility in female mice exposed transplacentally to diethylstilbestrol (DES). Fertil Steril. 1982; 38: 364–71.
62 Newbold RR. Lessons learned from perinatal exposure to diethylstilbestrol. Toxicol Appl Pharmacol. 2004; 199: 142–50.
63 McLachlan JA. Environmental signaling: what embryos and evolution teach us about endocrine disrupting chemicals. Endocr Res. 2001; 22: 319–41.
64 Li S, Hursting SD, Dzvis BJ, McLachlan JA, Barrett JC. Environmental exposure, DNA methylation, and gene regulation. Lessons from diethylstilbestrol-induced cancers. Ann NY Acad Sci. 2003; 983: 161–9.
65 Gray Nelson K, Sakai Y, Eitzman B, Steed T, McLachlan J. Exposure to diethylstilbestrol during a critical development period of the mouse reproductive tract leads to persistent induction of two estrogen-related genes. Cell Growth Differ. 1994; 5: 595–606.
66 McLachlan JA, Burow M, Chiang T-C, Li SF. Gene imprinting in developmental toxicology: a possible interface between physiology and pathology. Toxicol Lett. 2001; 120: 161–4.
67 Couse JF, Dixon D, Yates M, Moore AB, Ma L, Maas R, Korach KS. Estrogen receptor-α knockout mice exhibit resistance to the developmental effects of neonatal diethylstilbestrol exposure on the female reproductive tract. Dev Biol. 2001; 238: 224–38.
68 Mericskay M, Carta L, Sassoon D. Diethylstilbestrol exposure *in utero*: A paradigm for mechanisms leading to adult disease. Birth Defects Res A Clin Mol Teratol. 2005; 73: 133–5.
69 Kamiya K, Sato T, Nishimura N, Goto Y, Kano K, Iguchi T. Expression of estrogen receptor and proto-oncogene messenger ribonucleic acids in reproductive tracts of ne-

onatally diethylstilbestrol-exposed female mice with or without post-pubertal estrogen administration. Exp Clin Endocrinol Diabetes. 1996; 104: 111–22.

70 Yamashita S, Takayanagi A, Shimizu N. Effects of neonatal diethylstilbestrol exposure on c-fos and c-jun protooncogene expression in the mouse uterus. Histol Histopathol. 2001; 16: 131–40.

71 Falck L, Forsberg J-G. Immunohistochemical studies on the expression and estrogen dependency of EGF and its receptor and C-fos proto-oncogene in the uterus and vagina of normal and neonatally estrogen-treated mice. Anat Rec. 1996; 245: 459–71.

72 Ma L, Benson GV, Lim H, Dey SK, Maas RL. Abdominal B (abdB) Hoxa genes: regulation in adult uterus by estrogen and progesterone and repression in müllerian duct by the synthetic estrogen diethylstilbestrol (DES). Dev Biol. 1998; 197: 141–54.

73 Block K, Kardana A, Igarashi P, Taylor HS. *In utero* diethylstilbestrol (DES) exposure alters Hox gene expression in the developing müllerian system. FASEB. 2000; J 4: 1101–8.

74 SatoT, Ohta Y, Okamura H, Hayashi S, Iguchi T. Estrogen receptor (ER) and its messenger ribonucleic acid expression in the genital tract of female mice exposed neonatally to tamoxifen and diethylstilbestrol. Anat Rec. 1996; 44: 374–85.

75 Okada A, Sato T, Ohta Y, Buchanan DL, Iguchi T. Effect of diethylstilbestrol on cell proliferation and expression of epidermal growth factor in the developing female rat reproductive tract. J Endocrinol. 2001; 170: 539–54.

76 Bestor TH. The DNA methyltransferases of mammals. Hum Mol Genet. 2000; 9: 2395–402.

77 Sakai Y, Suetake I, Itoh K, Mizugaki M, Tajima S, Yamashita S. Expression of DNA methyltransferase (Dnmt1) in testicular germ cells during development of mouse embryo. Cell Struct Function. 2001; 26: 685–91.

78 La Salle S, Trasler JM. Dynamic expression of DNMT3a and DNMT3b isoforms during male germ cell development in the mouse. Dev Biol. 2006; 296: 71–82.

79 Sakai Y, Suetake I, Shinozaki F, Yamashina S, Tajima S. Co-expression of de novo DNA methyltransferases Dnmt3a2 and Dnmt3L in gonocytes of mouse embryos. Gene Expression Patterns. 2004; 5: 231–7.

80 Spearow JL, Doemeny P, Sera R, Leffler R, Barkley M. Genetic variation in susceptibility to endocrine disruption by estrogen in mice. Science. 1999; 285: 1259–61.

81 Wu Q, Ohsako S, Ishimura R, Suzuki JS, Tohyama C. Exposure of mouse preimplantation embryos to 2,3,7,8-tetrachlorodibenzo-*p*-dioxin (TCDD) alters the methylation status of imprinted genes *H19* and *Igf2*. Biol Reprod. 2004; 70: 1790–7.

82 Fukata H, Mori C. Epigenetic alteration by the chemical substances, food and environmental factors. Reprod Med Biol. 2004; 3: 115–21.

The American Journal of Pathology, Vol. 180, No. 1, January 2012

DOI: 10.1016/j.ajpath.2011.09.027

Immunopathology and Infectious Diseases

CCR7 with $S1P_1$ Signaling through AP-1 for Migration of $Foxp3^+$ Regulatory T-Cells Controls Autoimmune Exocrinopathy

Naozumi Ishimaru,* Akiko Yamada,*
Takeshi Nitta,† Rieko Arakaki,* Martin Lipp,‡
Yousuke Takahama,† and Yoshio Hayashi*

From the Department of Oral Molecular Pathology, Institute of Health Biosciences, The University of Tokushima Graduate School, Tokushima, Japan; the Department of Experimental Immunology,† Institute for Genome Research, The University of Tokushima, Tokushima, Japan; and the Department of Molecular Tumor Genetics and Immunogenetics,‡ Max-Delbruck Center for Molecular Medicine, Berlin, Germany*

Forkhead box p3-positive ($Foxp3^+$) regulatory T cells (T_{reg} cells) participate in maintaining peripheral immune tolerance and suppressing autoimmunity. We recently reported that *in situ* patrolling by C-C-chemokine receptor 7 $(CCR7)^+$ T_{reg} cells in target organs is essential for controlling autoimmune lesions in Sjögren's syndrome. In the present study, the molecular mechanism underlying CCR7-mediated T_{reg} cell migration was investigated in a mouse model. The impaired migratory response of $Ccr7^{-/-}$ T_{reg} cells to sphingosine 1-phosphate (S1P) occurred because of defective association of S1P receptor 1 ($S1P_1$) with a G coupled–protein. In addition, T-cell receptor (TCR)- and $S1P_1$-mediated Ras-related C3 botulinum toxin substrate 1 (Rac-1), extracellular signal-related kinase (ERK), and c-Jun phosphorylation required for activator protein 1 (AP-1) transcriptional activity were significantly impaired in $Ccr7^{-/-}$ T_{reg} cells. Surprisingly, the abnormal nuclear localization of Foxp3 was detected after abrogation of the c-Jun and Foxp3 interaction in the nucleus of $Ccr7^{-/-}$ T_{reg} cells. These results indicate that CCR7 essentially controls the migratory function of T_{reg} cells through $S1P_1$-mediated AP-1 signaling, which is regulated through its interaction with Foxp3 in the nucleus. *(Am J Pathol 2012, 180: 199–208; DOI: 10.1016/j.ajpath.2011.09.027)*

Regulatory T cells (T_{reg} cells) are a unique subset of T cells that play a critical role in maintaining immune tolerance.[1–3] The expression of the transcription factor forkhead box p3 (Foxp3) is the genetic hallmark of T_{reg} cells.[4–6] Foxp3-targeted genes in T_{reg} cells are up-regulated or down-regulated, suggesting that Foxp3 functions as both a transcriptional activator and a repressor.[7] Previous evidence indicates that Foxp3 controls T_{reg} functions by interacting with multiple transcription factors.[8] The function or expression of Foxp3 is controlled through complexes formed with other transcription factors, such as nuclear factor of activated T cells (NFAT), RUNX1/acute myelogenous leukemia (AML) 1, and nuclear factor kappa-B (NF-κB).[9,10] In addition, Foxp3 can maintain T_{reg} cell unresponsiveness (anergy) by selectively inhibiting the promoter DNA-binding activity of activator protein 1 (AP-1).[11] However, the molecular mechanism by which Foxp3 switches between transcriptional activation and repression in T_{reg} cells has not been well defined.

Previously, we reported autoimmune exocrinopathy in salivary and lacrimal glands resembling Sjögren's syndrome in C-C-chemokine receptor 7 (CCR7)-deficient ($Ccr7^{-/-}$) mice.[12] Enhanced immunity in $Ccr7^{-/-}$ mice is caused by defective lymph node (LN) positioning of T_{reg} cells and consequent impairment of suppressor function.[13] In a recent report, we demonstrated that CCR7 essentially governs the patrolling functions of T_{reg} cells by controlling their migration to target organs to maintain autoimmunity.[14] Furthermore, we found that the migratory function of $Ccr7^{-/-}$ T_{reg} cells in response to sphingosine 1-phosphate (S1P) was impaired, suggesting that CCR7

Supported by Funding Program for Next Generation World-Leading Researchers in Japan (LS090), Grants-in-Aid for Scientific Research (no. 17109016 and 17689049) from the Ministry of Education, Science, Sport, and Culture of Japan, and by funds from the Uehara Memorial Foundation and the Takeda Science Foundation (N.I.).

Accepted for publication September 13, 2011.

Supplemental material for this article can be found at *http://ajp.amjpathol.org* or at doi: 10.1016/j.ajpath.2011.09.027.

Address reprint requests to Naozumi Ishimaru, D.D.S., Ph.D., Department of Oral Molecular Pathology, Institute of Health Biosciences, The University of Tokushima Graduate School, 3-18-15 Kuramotocho, Tokushima 770-8504, Japan. E-mail: ishimaru@dent.tokusghima-u.ac.jp.

participates in the molecular mechanism underlying the migratory function of peripheral T_{reg} cells through S1P and one of its receptors, $S1P_1$.[14] In contrast, at the molecular level, T_{reg} cells in $S1P_1$-deficient mice were found to be defective in egress from the thymus; the number of peripheral T_{reg} cells in $S1P_1$-deficient mice was also increased, compared with peripheral T_{reg} cells in control mice.[15] Furthermore, $S1P_1$ transgenic mice developed autoimmune lesions because of a decrease in the number of T_{reg} cells in the thymus.[15] The S1P-$S1P_1$ axis is thus believed to play an important role in restraining the development and function of $Foxp3^+$ T_{reg} cells.

Mitogen-activated protein kinase (MAPK) signaling and AP-1 components are crucial in $S1P_1$ signaling in peripheral T cells.[16] In addition, the function of T_{reg} cells can be regulated by Foxp3 binding to phosphorylated c-Jun, thereby controlling AP-1 transcriptional activity.[11] Although the relationship between CCR7 and S1P/$S1P_1$ signaling in peripheral T_{reg} cells has not been clarified, it is possible that interactions among several molecules (including CCR7, S1P/$S1P_1$, and Foxp3) play a critical role in controlling the migratory response of peripheral T_{reg} cells.

In the present study, analysis of defective T_{reg} cells in *Ccr7*$^{-/-}$ mice revealed a novel regulation of Foxp3 nuclear localization that controls $S1P_1$-mediated AP-1 signaling after T_{reg} cell migration.

Materials and Methods

Mice

Ccr7$^{-/-}$, *Ccr7*$^{+/+}$ and C57BL/6 mice were reared in our specific pathogen-free mouse colony. Mice were provided food and water *ad libitum*. Experiments were humanely conducted under the regulation and permission of the Animal Care and Use Committee of the University of Tokushima (Tokushima, Japan).

Histological Analysis

All organs were removed from mice, fixed with 10% phosphate-buffered formaldehyde (pH 7.2), and prepared for histological examination. Sections were stained with H&E.

Cell Preparation

T_{reg} cells and $CD25^-CD4^+$ cells were enriched from LNs. In brief, $CD4^+$ cells were prepared using anti-B220, CD8, MHC class II, and NK1.1 monoclonal antibodies (mAbs) (eBioscience, San Diego, CA) and magnetic beads (Dynal Biotech, Oslo, Norway). $CD25^+CD4^+$ or $CD25^-CD4^+$ cells were enriched using biotin-conjugated anti-CD25 mAb, magnetic beads, and a CELLection biotin binder kit (Dynal Biotech) or a regulatory T cell isolation kit (Miltenyi Biotec, Auburn, CA). The enriched $CD25^+CD4^+$ cells were confirmed to be approximately 90% $Foxp3^+$.

In Vitro *Suppression Assay*

For suppression assays, a total of 5×10^4 $CD25^-CD4^+$ T cells from C57BL/6 mice were stimulated with plate-coated anti-CD3 mAb (0.5 μg/mL) for 72 hours together with 1.25, 2.5, and 5×10^4 $CD25^+CD4^+$ T cells from the LNs of wild-type (WT) and *Ccr7*$^{-/-}$ mice. [^{3}H]-Thymidine incorporation during the last 12 hours of the culture for 72 hours was evaluated using an automated liquid scintillation β counter (Hitachi Aloka Medical, Ltd., Tokyo, Japan).

ELISA

For detection of IL-4, IL-10, and TGF-β, $CD25^+CD4^+$ T cells were stimulated with plate-coated anti-CD3 mAb for 24 hours. The supernatants were added to microtiter plates precoated with an antibody specific for IL-4, IL-10, and TGF-β. The biotinylated antibody was added, and the plate was incubated for 2 hours at room temperature. After a wash, streptavidin-horseradish peroxidase solution was added to each well and the plate was incubated for 30 minutes. Finally, stabilized chromogen substrate was added to each well, and the absorbance of each well was read at 450 nm using an automated microplate reader (Bio-Rad Laboratories, Hercules, CA). Cytokine concentrations were obtained according to standard curves.

Confocal Microscopic Analysis

Cells were deposited onto poly-L-lysine-coated glass slides, and spun in a cytospin centrifuge. Sections were stained with 1 μg/mL of primary antibodies against phosphorylated ERK1/2, phosphorylated c-Jun (BD Biosciences, San Jose, CA), phosphorylated Rac-1 (Cell Signaling Technology, Danvers, MA), and Foxp3 (eBioscience, San Diego, CA) for 1 hour. After three washes in PBS, sections were stained with Alexa Fluor 568 donkey anti-rat IgG (H+L) (Molecular Probes; Invitrogen, Carlsbad, CA) or Alexa Fluor 488 horse anti-rabbit IgG (H+L) secondary antibodies for 30 minutes and washed with PBS. The nuclei were stained with DAPI. Sections were visualized with a laser scanning confocal microscope (Carl Zeiss MicroImaging, Göttingen, Germany). A 63×/1.4 oil differential interference contrast (DIC) objective lens was used. Quick Operation software, version 3.2 (Carl Zeiss), was used for image acquisition and Adobe Photoshop CS2 software (Adobe System, San Jose, CA) was used for image processing. Nuclear localization of Foxp3 and DAPI was evaluated within the imaging system.

Real-Time Quantitative RT-PCR

Total RNA was extracted from the T_{reg} cells of WT and *Ccr7*$^{-/-}$ mice with ISOGEN (Wako Pure Chemical, Osaka, Japan) and was then reverse-transcribed. Transcript levels of Gi, Rac-1, Foxp3, and β-actin were analyzed using the DNA engine OPTICOM system (Bio-Rad Laboratories) with SYBR Premix Ex Tag (Takara, Kyoto,

Japan). Primer sequences were as follows: Gi forward, 5′-TTTCTCTGGATGGGATGAGG-3′ and reverse, 5′-CCGAACCTCATGTTGTGTTG-3′; Rac-1 forward, 5′-GCCACTCAACGAGAGCCTAC-3′ and reverse, 5′-TCGGTTCTCCAGCTTGACTT-3′; Foxp3 forward, 5′-CCCAGGAAAGACAGCAACCTT-3′ and reverse, 5′-TTCTCACAACCAGGCCACTTG-3′; and β-actin forward, 5′-AAATCTGGCACCACACCTTC-3′ and reverse, 5′-GAGGCGTACAGGGATAGCA-3′.

Cell Culture and Migration Assay

For cell culturing with S1P or chemokines, cells were incubated in RPMI 1640 medium without fetal calf serum in the presence of S1P (0 to 100 nmol/L), CCL19 (100 ng/mL), or CCL21 (100 ng/mL) with plate-coated anti-CD3 mAb (0.5 μg/mL) for 3 to 12 hours. To evaluate chemotaxis by S1P, CCL19, or CCL21 in the T_{reg} cells of WT and *Ccr7*$^{-/-}$ mice, a Cultrex 96-well cell migration assay kit (Trevigen, Gaithersburg, MD) was used according to the manufacturer's instructions. Before the assay, the cells were starved for 24 hours in serum-free medium and incubated in RPMI 1640 without fetal calf serum. In addition, the cells were pretreated with inhibitors, including FTY720 (BioVision, San Francisco, CA), PTX, rapamycin, SB203580, and PD98059 (Sigma-Aldrich, St. Louis, MO) for 6 to 12 hours, and then the migration assay was performed.

Western Blotting and Immunoprecipitation

Whole-cell extracts of T_{reg} cells were prepared using a Pierce M-PER mammalian protein extraction kit (Thermo Fisher Scientific, Rockford, IL) or nuclear/cytosol fraction kit (BioVision). A total of 10 μg of each sample per well was applied to each well and was electrophoresed on 10% SDS-PAGE. Thereafter, the protein was electrophoretically transferred onto polyvinylidene difluoride membranes. Blocked membranes were incubated with antibodies specific for $S1P_1$ (Cayman Chemical, Ann Arbor, MI), Rac-1, phosphorylated Rac-1 (Cell Signaling Technology), Gi (Millipore-Chemicon International, Temecula, CA), phospho-c-Jun (BD Biosciences), total c-Jun (BD Biosciences), or glyceraldehyde-3-phosphate dehydrogenase (GAPDH; Santa Cruz Biotechnology, Santa Cruz, CA). Horseradish peroxidase-conjugated rabbit or mouse IgG was used as the secondary antibody. Protein binding was visualized using Amersham ECL Western blotting detection reagents (GE Healthcare, Piscataway, NJ). To quantify protein expression, the chemiluminescence image was analyzed using a ChemiDoc XRS system (Bio-Rad Laboratories). For immunoprecipitation, purified proteins captured with anti-Foxp3 mAb were incubated with Dynabeads protein G (Invitrogen). To remove genomic DNA, proteins were treated with DNase I. Precipitated proteins were analyzed by immunoblotting with anti-c-Jun or anti-Foxp3 (e-Bioscience) antibody.

c-Jun Transcriptional Activity

The transcriptional activity of c-Jun in the nuclear extracts from T_{reg} of WT and *Ccr7*$^{-/-}$ mice was analyzed using an Upstate c-Jun transcription factor assay kit (Millipore, Billerica, MA). In brief, nuclear extracts were incubated with a biotinylated double-stranded oligonucleotide probe containing the consensus sequence for c-Jun on a streptavidin-coated plate. Captured complexes were incubated with c-Jun antibody, horseradish peroxidase-conjugated secondary antibody, and tetramethylbenzidine substrate. The absorbance of samples was measured using an automated microplate reader at 450 nm.

Statistical Analysis

Student's *t*-test was used for statistical analysis. A *P* value of <0.05 was considered statistically significant.

Results

Relationship between Autoimmune Lesions and T_{reg} Cells in Ccr7$^{-/-}$ *Mice*

We found a significantly reduced proportion of Foxp3$^+$ T_{reg} cells in target organs, including the salivary and lacrimal glands, of *Ccr7*$^{-/-}$ mice, compared with *Ccr7*$^{+/+}$ mice, at approximately 3 months of age. This led to significantly increased retention of T_{reg} cells in the LNs of *Ccr7*$^{-/-}$ mice until mice were 6 months of age.[14] However, it is unclear whether the proportion of T_{reg} cells in target organs and LNs changed with aging during these 6 months. More severe autoimmune lesions in lacrimal glands of *Ccr7*$^{-/-}$ mice were observed at 9 and 18 months of age (Figure 1A). At 18 months of age, extensive infiltration of lymphocytes with destruction of exocrine gland cells was detected in *Ccr7*$^{-/-}$ mice (Figure 1A). The proportion of Foxp3$^+$ CD4$^+$ T_{reg} cells in the cervical LNs of *Ccr7*$^{-/-}$ mice was significantly increased, compared with WT mice, until 18 months of age (Figure 1B). The retention of T_{reg} cells in the LNs of *Ccr7*$^{-/-}$ mice increased with aging. In contrast, the proportion of T_{reg} cells in lacrimal glands of *Ccr7*$^{-/-}$ mice was significantly reduced, compared with *Ccr7*$^{+/+}$ mice (Figure 1C). In addition, although the absolute number of T_{reg} cells in the cervical LNs of normal mice decreased with aging, the number of LN T_{reg} cells in *Ccr7*$^{-/-}$ mice increased (Figure 1D). At 3 and 9 months of age, the cell number in T_{reg} cells in *Ccr7*$^{-/-}$ mice was significantly reduced, compared with control mice (Figure 1D). At 18 months of age, the number of cells of *Ccr7*$^{-/-}$ mice was similar to that of control mice (Figure 1D). Given that the total cell number in the LNs of *Ccr7*$^{-/-}$ mice significantly decreased, compared with control mice, the proportion of T_{reg} cells from *Ccr7*$^{-/-}$ mice was higher than that from control mice (Figure 1B). In contrast, the number of T_{reg} cells in lacrimal glands of *Ccr7*$^{-/-}$ mice were significantly reduced, compared with control mice (Figure 1E). These findings are consistent with our previous report that Foxp3$^+$ CD4$^+$

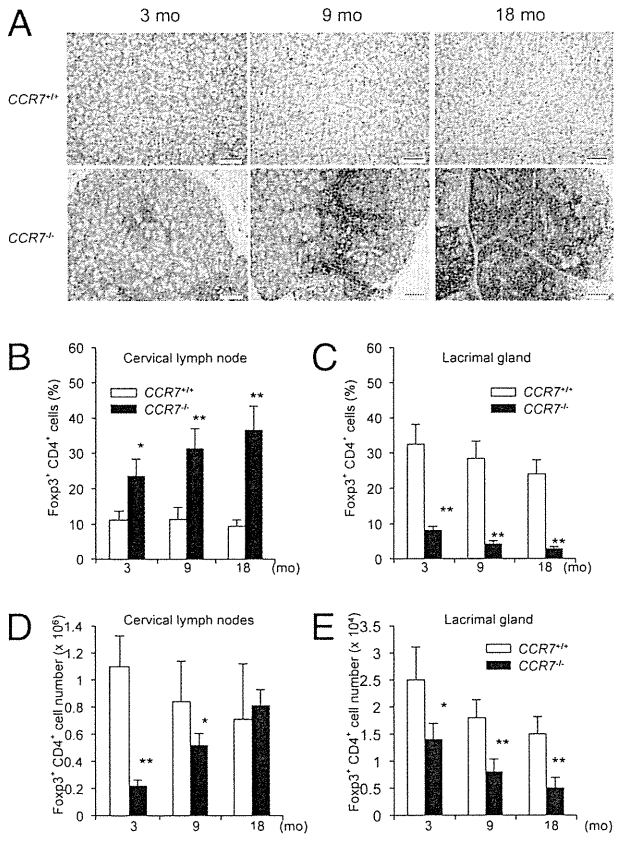

Figure 1. Autoimmune exocrinopathy and T_{reg} cell in *Ccr7*$^{-/-}$ mice. **A:** Histology of lacrimal glands of *Ccr7*$^{+/+}$ and *Ccr7*$^{-/-}$ mice at 3, 9, and 18 months of age. H&E staining was performed on paraffin-embedded sections. Images are representative of 5 to 7 mice per group. Scale bars = 500 μm. **B:** The proportions of Foxp3$^+$ CD4$^+$ T_{reg} cells in cervical LNs in *Ccr7*$^{+/+}$ and *Ccr7*$^{-/-}$ mice at 3, 9, and 18 months of age were detected by flow cytometric analysis. **C:** The proportions of Foxp3$^+$ CD4$^+$ T_{reg} cells in lacrimal glands of *Ccr7*$^{+/+}$ and *Ccr7*$^{-/-}$ mice at 3, 9, and 18 months of age were detected by flow cytometric analysis. **D:** Quantification of Foxp3$^+$ CD4$^+$ T_{reg} cells in cervical LNs of *Ccr7*$^{+/+}$ and *Ccr7*$^{-/-}$ mice at 3, 9, and 18 months of age. **E:** Quantification of Foxp3$^+$ CD4$^+$ T_{reg} cells in lacrimal glands of *Ccr7*$^{+/+}$ and *Ccr7*$^{-/-}$ mice at 3, 9, and 18 months of age. Results are presented as means ± SD for five mice in each group. $^*P < 0.05$; $^{**}P < 0.005$ versus WT.

T_{reg} cell numbers are significantly reduced in target organs, such as salivary or lacrimal glands, in *Ccr7*$^{-/-}$ mice and in patients with Sjögren's syndrome.[14]

Chemotactic Response to S1P and Suppressive Function of Ccr7$^{-/-}$ *T_{reg} Cells*

We examined in *vitro* chemotactic responses of CD4$^+$ T cells from WT and *Ccr7*$^{-/-}$ mice in response to S1P. In both WT and *Ccr7*$^{-/-}$ mice, no migratory responses of CD25$^+$CD4$^+$ T_{reg} cells were observed with the addition of S1P (Figure 2A). Although there was a small increase in the chemotactic response of WT and *Ccr7*$^{-/-}$ CD25$^-$CD4$^+$ T cells to S1P, there were no differences in the response between WT and *Ccr7*$^{-/-}$ mice (Figure 2B). Next, we examined the chemotactic response of anti-CD3 mAb-engaged *Ccr7*$^{-/-}$ CD4$^+$ cells to S1P, and found that the migratory response of *Ccr7*$^{-/-}$ T_{reg} cells to S1P was significantly impaired, compared with WT T_{reg} cells (Figure 2C). In contrast, the response of CD25$^-$CD4$^+$ cells of *Ccr7*$^{-/-}$ mice was not impaired (Figure 2D). These findings suggest that the chemotactic response of T cells to S1P is dependent on T-cell receptor/CD3 signaling.

To determine whether there were migratory responses to chemoattractants other than S1P, we performed migration assays using IL-6 and MIP-2, and found no difference in the migration activity between WT and *CCR7*$^{-/-}$ T_{reg} cells. The results for anti-CD3 mAb-engaged T_{reg} cells are shown in Figure 2, E and F. Moreover, there were also no differences in migration activity in response to IL-6 and MIP-2 between unstimulated WT and *CCR7*$^{-/-}$ T_{reg} cells (data not shown). In contrast, when we examined the *in vitro* suppressive function of *Ccr7*$^{-/-}$ T_{reg} cells, we found that the suppression of *Ccr7*$^{-/-}$ T_{reg} cells on the proliferative response elicited by the anti-CD3 mAb in normal CD25$^-$CD4$^+$ cells from C57BL/6 mice was similar to that of WT T_{reg} cells (Figure 2G). In addition, there were no differences in the production of suppressive cytokines such as IL-4, IL-10, or TGF-β in *Ccr7*$^{-/-}$ or WT T_{reg} cells (Figure 2H). These findings suggest that CCR7 signaling controls the migration of T_{reg} cells, but does not control the suppressive function of T_{reg} cells. This is consistent with the failure of *in vivo* migration to target organs in *Ccr7*$^{-/-}$ T_{reg} cells.[14]

Activation of Signaling Molecules Downstream of S1P$_1$ in Ccr7$^{-/-}$ *T_{reg} Cells*

S1P$_1$, one of receptors for S1P, is expressed on the cell surface and is known to be internalized when the S1P ligand binds to S1P$_1$ after activation of the signaling molecules required for the migratory response.[17] We detected expression of S1P$_1$ in WT and *Ccr7*$^{-/-}$ T_{reg} cells by Western blotting with anti-S1P$_1$ polyclonal antibodies. There was no difference in S1P$_1$ expression between WT and *Ccr7*$^{-/-}$ T_{reg} cells (Figure 3, A and B). S1P$_1$ has been shown to signal exclusively through the heterotrimeric G protein Gi.[18] We therefore used Western blotting to evaluate Gi expression in WT and *Ccr7*$^{-/-}$ T_{reg} cells after anti-CD3 mAb and S1P treatment (see Supplemental Figure S1A at *http://ajp.amjpathol.org*). There were no differences in expression between WT and *Ccr7*$^{-/-}$ T_{reg} cells, and this was unchanged by stimulus (see Supplemental Figure S1A at *http://ajp.amjpathol.org*).

The phosphorylation of Rac-1,[19] a key molecule downstream of G-protein signaling, was observed in WT T_{reg} cells but not in *Ccr7*$^{-/-}$ T_{reg} cells stimulated with the anti-CD3 mAb and S1P (Figure 3C). Phosphorylation of Rac-1 was evaluated by Western blotting. The phosphorylation of Rac-1 in WT T_{reg} cells was detectable after CD3 engagement, and the addition of S1P enhanced Rac-1 phosphorylation in anti-CD3 mAb-stimulated T_{reg} cells (Figure 3D). In contrast, the phosphorylation of Rac-1 in *Ccr7*$^{-/-}$ T_{reg} cells was low, compared with that in WT T_{reg} cells (Figure 3D). In contrast, there was no difference in Rac-1 phosphorylation between WT and *Ccr7*$^{-/-}$ CD25$^-$CD4$^+$ T cells (see Supplemental Figure S2 at *http://ajp.amjpathol.org*). These findings demonstrate the impairment of the signaling pathway in *Ccr7*$^{-/-}$ T_{reg} cells.

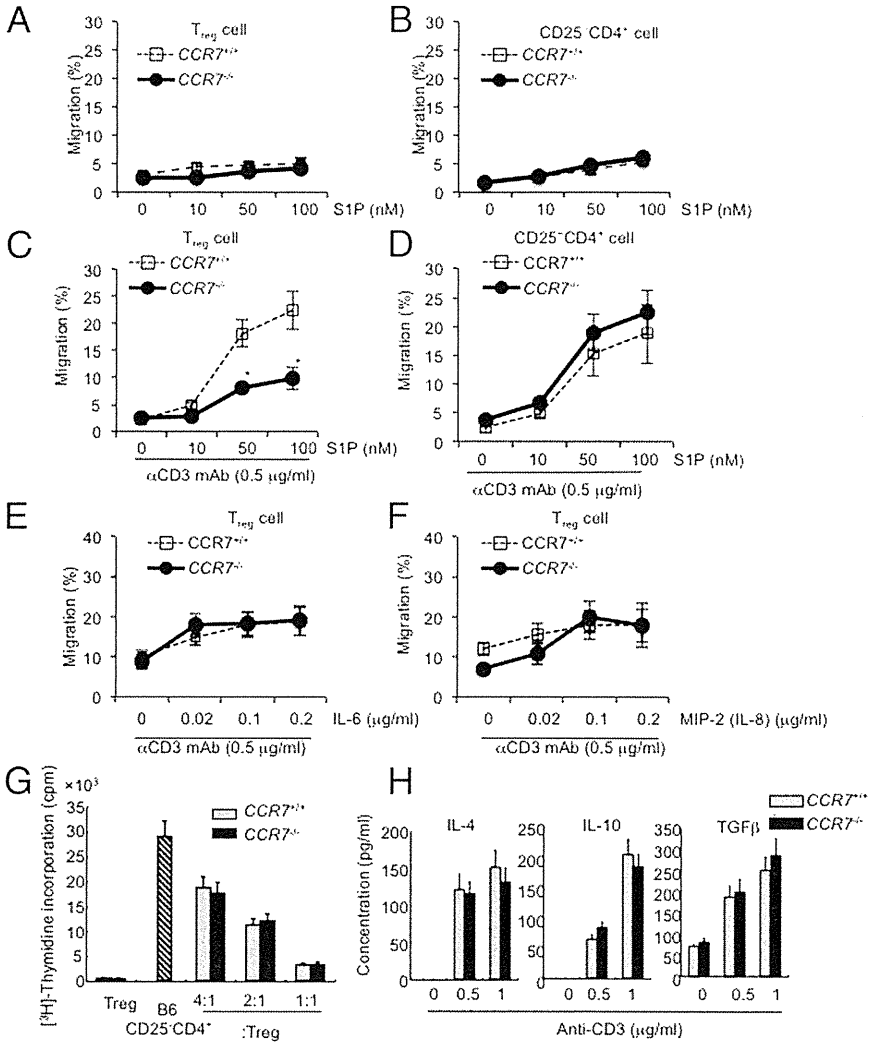

Figure 2. Signaling pathway in *Ccr7*$^{-/-}$ T_{reg} cells. **A** and **B:** Migration assay of T_{reg} cells (**A**) and $CD25^{-}CD4^{+}$ T cells (**B**) from LNs of WT and *Ccr7*$^{-/-}$ mice in response to S1P (0 to 100 nmol/L) was performed using purified T_{reg} and $CD25^{-}CD4^{+}$ T cells for 12 hours. **C** and **D:** Migration assay of T_{reg} cells (**C**) and $CD25^{-}CD4^{+}$ T cells (**D**) from LNs of WT and *Ccr7*$^{-/-}$ mice in response to S1P (0 to 100 nmol/L) was performed using anti-CD3mAb-stimulated T cells for 12 hours. **E:** Migratory response to IL-6 (0 to 0.2 μg/mL) in anti-CD3 mAb-stimulated T_{reg} cells. **F:** Migratory response to MIP-2 (0 to 0.2 μg/mL) in anti-CD3 mAb-stimulated T_{reg} cells. Data are presented as means ± SD (n = 3) and are representative of three independent experiments. **G:** *In vitro* suppression assays were performed by evaluation of the proliferative response in purified $CD25^{-}CD4^{+}$ T cells from C57BL/6 mice. $CD25^{-}CD4^{+}$ T cells were cocultured with WT or *Ccr7*$^{-/-}$ T_{reg} cells on anti-CD3 mAb-coated plates for 72 hours. The proliferative response was evaluated by incorporation of $[^{3}H]$-thymidine during the last 18 hours of incubation. Data are presented as means ± SD (n = 3) and are representative of three independent experiments. **H:** WT or *Ccr7*$^{-/-}$ T_{reg} cells were stimulated with anti-CD3 mAb for 24 hours. Concentrations of IL-4, IL-10, and TGF-β in the culture supernatants were measured by enzyme-linked immunosorbent assay. Data are presented as means ± SD (n = 3) and are representative of two independent experiments.

Next, we focused on examining migratory function and CCR7 signaling using a Gi protein inhibitor, pertussis toxin (PTX), and an S1P receptor agonist, FTY720 (Figure 3E). The increased migratory response of WT T_{reg} cells on stimulation with anti-CD3 mAb and S1P was reduced by pretreatment with FTY720 or PTX (Figure 3E). Moreover, when WT T_{reg} cells were incubated with a CCR7 ligand (either CCL19 or CCL21) in addition to anti-CD3 mAb and S1P, migratory responses were significantly enhanced in contrast to the response to anti-CD3 mAb and S1P (Figure 3E). These enhanced responses were reduced with pretreatment of FTY720 and PTX to the levels of *Ccr7*$^{-/-}$ T_{reg} cells (Figure 3E). This result suggests that CCR7 signaling in T_{reg} cells is dependent on cooperation with $S1P/S1P_1$ and Gi, in addition to CD3 signaling.

MAPK Signaling in Ccr7$^{-/-}$ *T_{reg} Cells*

To further elucidate the importance of $S1P_1$ signaling for T_{reg} cell egress, we analyzed MAPK signaling and the AP-1 components that play crucial roles in $S1P_1$ signaling in T cells.[16] Phosphorylation of ERK after stimulation with anti-CD3 mAb and S1P was observed in WT T_{reg} cells, but not in *Ccr7*$^{-/-}$ T_{reg} cells (Figure 4A), and this phosphorylation was enhanced with addition of S1P (Figure 4B). To determine whether this signaling was through MAPK or Akt-mTOR, we performed migration assays using the mTOR inhibitor rapamycin and two MAPK inhibitors. The migratory activity of WT T_{reg} cells increased with treatment of anti-CD3 mAb and S1P, and was not fully inhibited by pretreatment with rapamycin (Figure 4C). The increased migratory response of WT T_{reg} cells was significantly inhibited by the addition of the ERK MAPK inhibitor PD98059, but not by the addition of the p38 MAPK inhibitor SB203580 (Figure 4C). These findings suggest that CCR7-mediated ERK activation plays a crucial role in the migratory function of T_{reg} cells.

Association of c-Jun Activity with CCR7/$S1P_1$ Signaling

When T_{reg} cells of WT mice were stimulated with anti-CD3 mAb and S1P, phosphorylated c-Jun protein colocalized with Foxp3 in the nucleus. In contrast, phosphorylation of c-Jun was undetectable in *Ccr7*$^{-/-}$ T_{reg} cells stimulated

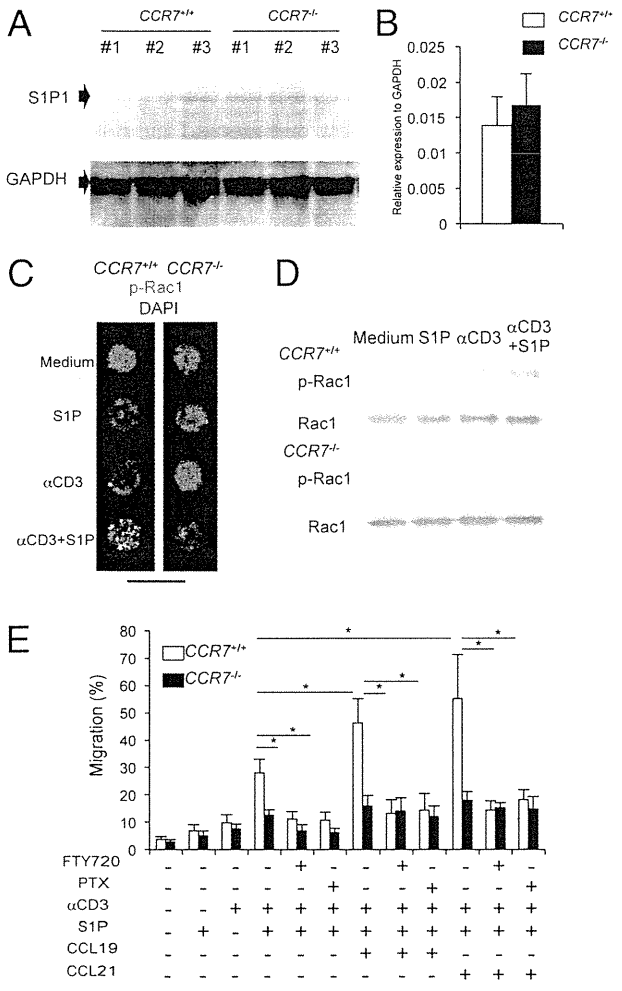

Figure 3. $S1P_1$ expression in $Ccr7^{-/-}$ T_{reg} cells. **A:** Western blotting of $S1P_1$ in T_{reg} cells from WT and $Ccr7^{-/-}$ mice (n = 3/group) was performed. GAPDH expression was used as a housekeeping protein. **B:** Relative expression of $S1P_1$ to GAPDH was quantified using the protein band intensities in A. Data are presented as means ± SD (n = 3). **C:** Phosphorylation of Rac-1 in T_{reg} cells of LNs from WT and $Ccr7^{-/-}$ mice was analyzed under confocal microscopy. Nuclei were stained with DAPI. Images are representative of three mice in each group. Scale bar =10 μm. **D:** Western blot analysis of Rac-1 and phosphorylated Rac-1 was performed. Results are representative of three independent experiments. **E:** Migration assay of WT and $Ccr7^{-/-}$ T_{reg} cells was performed using anti-CD3 mAb (0.5 mg/mL), S1P (100 nmol/L), CCL19 (50 ng/mL), CCL21 (50 ng/mL), and pretreatment (6 hours) with FTY720 or PTX. Data are presented as means ± SD (n = 3) and are representative of three independent experiments. $^*P < 0.05$.

with anti-CD3 mAb in the presence of S1P (Figure 5A). In support of these findings, the immunoblot analysis showed much stronger phosphorylation of c-Jun in WT T_{reg} cells stimulated with anti-CD3 mAb and S1P than in $Ccr7^{-/-}$ T_{reg} cells (Figure 5B). Furthermore, the transcriptional activity of c-Jun was significantly increased using nuclear extracts from WT T_{reg} cells stimulated with anti-CD3 mAb and S1P, compared with extracts from $Ccr7^{-/-}$ T_{reg} cells (Figure 5C). These results show that the CCR7-dependent TCR/CD3-S1P/$S1P_1$ signaling pathway is critical for T_{reg} function through AP-1 activation.

To examine whether the transcriptional activity of c-Jun is controlled by CCR7 ligands (CCL21 and CCL19), we analyzed the activity of WT T_{reg} cells stimulated with anti-CD3mAb in the presence of both S1P and CCL21 or CCL19. The transcriptional activity of c-Jun in anti-CD3mAb-engaged T_{reg} cells was enhanced by S1P and CCL21 or CCL19 (Figure 6, A and B). On the other hand, the transcriptional activity of c-Jun of $Ccr7^{-/-}$ T_{reg} cells was enhanced by CCR7 ligands, in addition to CD3 engagement and S1P (Figure 6, A and B). These results suggest that the cooperative action of CCR7 signaling with the TCR/CD3-S1P/$S1P_1$ signaling pathway plays an important role in the AP-1-mediated function of T_{reg} cells.

Abnormal Nuclear Localization of Foxp3 in Ccr7$^{-/-}$ T_{reg} Cells

As a unique finding regarding the localization of Foxp3 in $Ccr7^{-/-}$ T_{reg} cells, Foxp3 was positioned like a ring in the perinuclear region of unstimulated T_{reg} cells in $Ccr7^{-/-}$ mice, whereas in WT T_{reg} cells it was positioned in the center of the nucleus (Figure 5A). In further analysis using confocal microscopy, in $Ccr7^{-/-}$ mice Foxp3 was detected in the nuclear membrane and perinucleus, or a small amount of Foxp3 protein was detected in the cytoplasm near the nuclear membranes of LN T_{reg} cells,

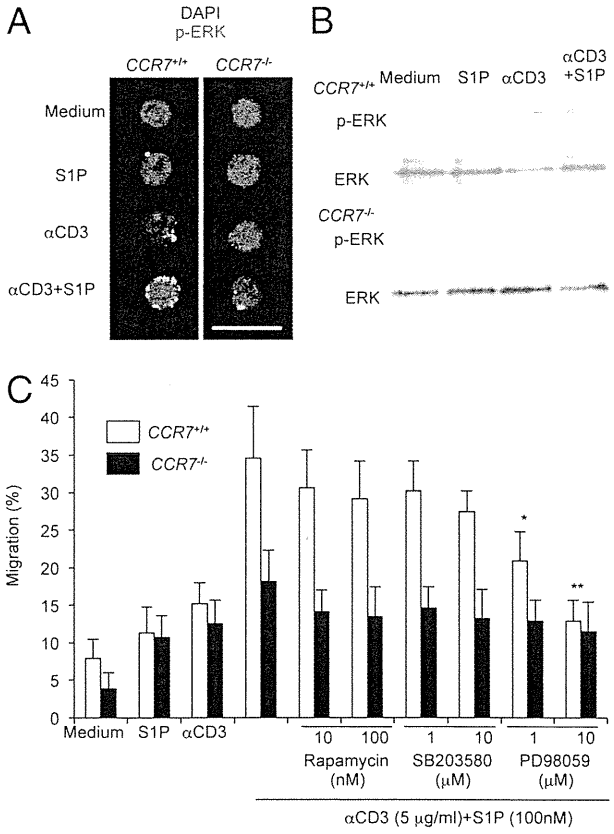

Figure 4. Signaling pathway downstream of $S1P_1$ in $Ccr7^{-/-}$ T_{reg} cells. **A:** Phosphorylation of ERK in $Foxp3^+$ T_{reg} cells of LNs from WT and $Ccr7^{-/-}$ mice was detected under confocal microscopy. Scale bar = 10 μm. **B:** Phosphorylation of ERK and total ERK in $Foxp3^+$ T_{reg} cells of LNs from WT and $Ccr7^{-/-}$ mice were detected by Western blotting. **C:** Migration assay of WT and $Ccr7^{-/-}$ T_{reg} cells was performed using anti-CD3 mAb (0.5 mg/mL), S1P (100 nmol/L), CCL19 (50 ng/mL), CCL21 (50 ng/mL), and pretreatment (6 hours) with rapamycin (10 and 100 nmol/L), SB203580 (1 and 10 μmol/L), or PD98059 (1 and 10 μmol/L). Data are presented as means ± SD (n = 3) and are representative of three independent experiments. $^*P < 0.05$; $^{**}P < 0.005$.

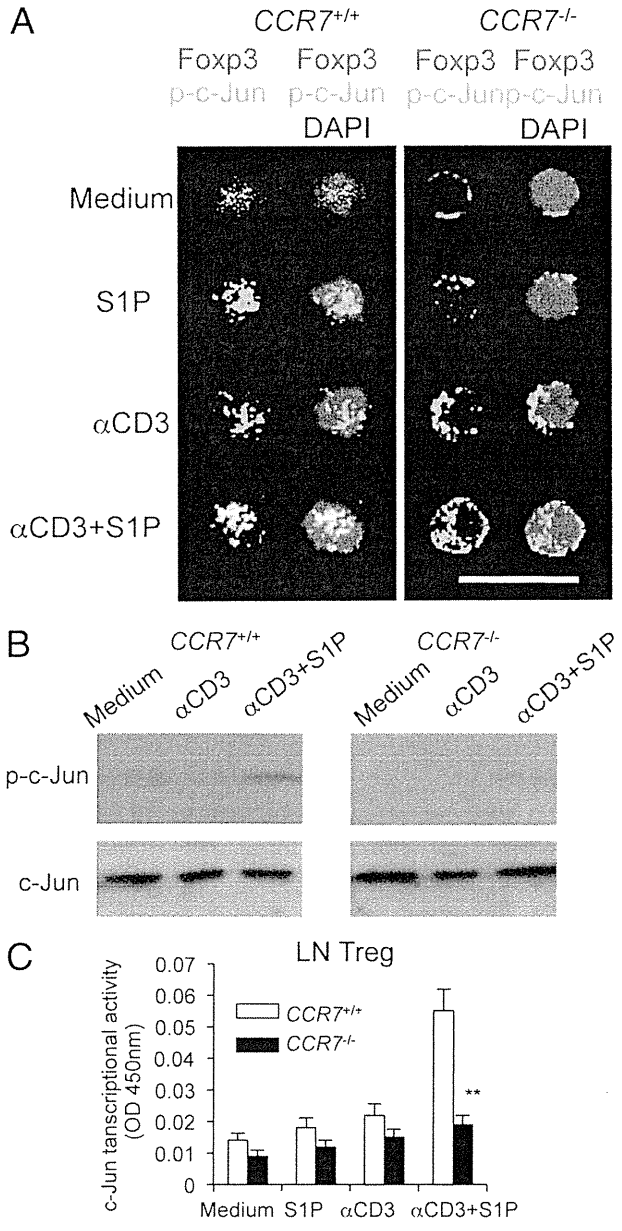

Figure 5. MAPK and AP-1 signaling in T_{reg} cells through $S1P_1$ and CCR7. **A:** Foxp3 and phospho-c-Jun in LN T_{reg} cells from WT and *Ccr7*$^{-/-}$ mice were analyzed under confocal microscopy. Nuclei were stained with DAPI. Results are representative of three independent experiments. Scale bar = 10 μm. **B:** Detection of phospho-c-Jun and total c-Jun in LN T_{reg} cells from WT and *Ccr7*$^{-/-}$ mice was analyzed by Western blot. Results are representative of two independent experiments. **C:** c-Jun transcriptional activity of LN T_{reg} cells from WT and *Ccr7*$^{-/-}$ mice was measured using an AP-1 binding probe. Data are presented as means ± SD (n = 3) and are representative of two independent experiments. $^{**}P < 0.005$ versus WT.

whereas in WT T_{reg} cells it was present exclusively in the nucleus (Figure 7, A and B). Even when *Ccr7*$^{-/-}$ T_{reg} cells were cultured without stimulus (medium only), Foxp3 was localized in the perinuclear region of the cell (Figure 5A,). When *Ccr7*$^{-/-}$ T_{reg} cells were stimulated with anti-CD3 mAb or anti-CD3 mAb + S1P, Foxp3 was localized both in the perinucleus and in the center of the nucleus (Figure 5A). These findings suggest that CCR7 regulates the nuclear localization of Foxp3. According to a recent report, Foxp3 significantly suppresses the transcriptional activity and promoter DNA binding of AP-1 by interacting with c-Jun, indicating that Foxp3 is a suppressor of c-Jun-based AP-1 transcriptional activity.[11] The binding of Foxp3 to c-Jun in WT T_{reg} cells stimulated by anti-CD3 mAb and S1P, was observed by immunoprecipitation with anti-Foxp3 mAb; however, this binding was not present in *Ccr7*$^{-/-}$ T_{reg} cells (Figure 7C). In contrast, there were no differences in mRNA expression of Foxp3 between WT and *Ccr7*$^{-/-}$ T_{reg} cells (Figure 7D). It is may be that Foxp3 is localized in the perinuclear region of the cells because of impaired c-Jun activation in *Ccr7*$^{-/-}$ T_{reg} cells.

Discussion

In the present study, we confirmed two possible molecular mechanisms underlying T_{reg} cell function mediated by CCR7. In one mechanism, our results suggest that the cooperative action of CCR7 with TCR/CD3 controls the internalization of S1P/$S1P_1$ with Gi after the phosphorylation of c-Jun as well as MAPK activation in T_{reg} cells (see Supplemental Figure S3 at *http://ajp.amjpathol.org*). The other mechanism shows that Foxp3 can bind to phosphorylated c-Jun in the nucleus to inhibit the transcriptional activity required for the migratory function or unresponsiveness of Treg cells. In contrast, c-Jun unbound from Foxp3 in the nucleus may act as a transcription factor for the migratory function of peripheral T_{reg} cells (see Supplemental Figure S3 at *http://ajp.amjpathol.org*). We hypothesize that the migratory function of T_{reg} cells is controlled by c-Jun activation, which is regulated by the S1P/$S1P_1$ pathway through the cooperative action between TCR/CD3 and CCR7 signaling and the molecular interaction of Foxp3 with c-Jun. In contrast, in *Ccr7*$^{-/-}$ T_{reg} cells, defective internalization of S1P/$S1P_1$ after ac-

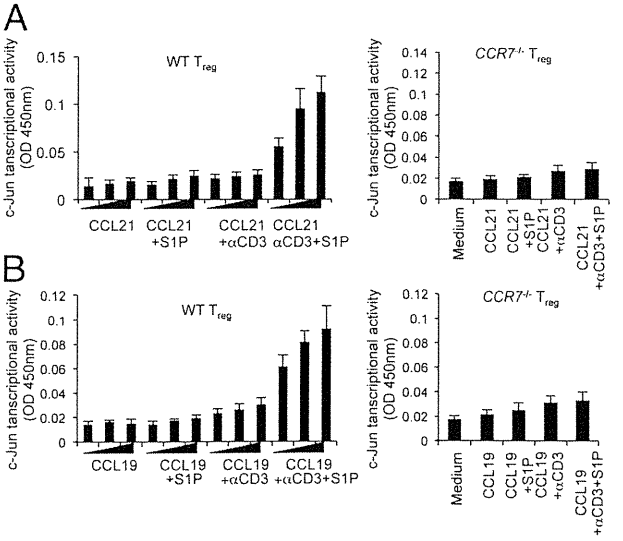

Figure 6. Control of c-Jun transcriptional activity in T_{reg} cells by ligation with CCR7. The c-Jun transcriptional activity of WT and *Ccr7*$^{-/-}$ T_{reg} cells stimulated with plate-coated anti-CD3mAb (0.5 μg/mL) in the presence of S1P and CCL21 (0, 20, 50 ng/mL) (**A**) or CCL19 (0, 20, 50 ng/mL) (**B**) was evaluated. For *Ccr7*$^{-/-}$ T_{reg} cells, CCL19 and CCL21 were used (50 ng/mL). Data are presented as means ± SD (n = 3) and are representative of two independent experiments. OD, optical density.

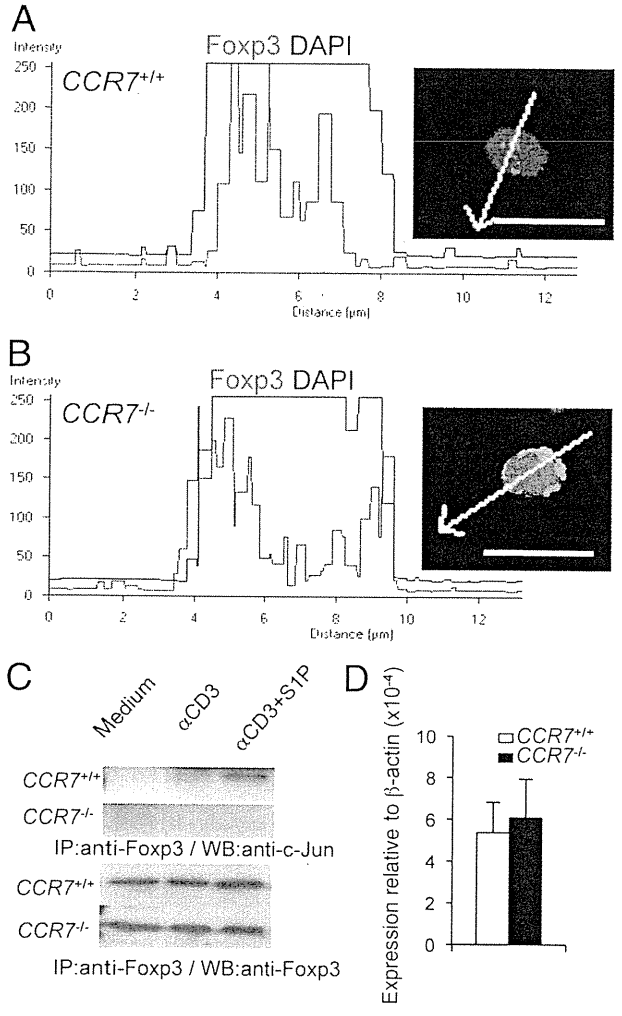

Figure 7. Abnormal nuclear localization of Foxp3 and impaired binding of Foxp3 to c-Jun. **A** and **B:** Nuclear localization of Foxp3 was evaluated by confocal microscopy analysis with DAPI staining. Relative fluorescence intensity of Foxp3 and DAPI along the axis of the arrow in the direction pointed by the arrow is shown. Results are representative of two independent experiments. Scale bars =10 μm. **C:** Impairment of interaction between Foxp3 and c-Jun in *Ccr7*$^{-/-}$ T_{reg} was detected by immunoprecipitation with anti-Foxp3 mAb and by Western blotting with anti-c-Jun pAb. Results are representative of two independent experiments. **D:** Foxp3 mRNA expression was quantified by real-time PCR. Data are presented as means ± SD (n = 3).

tivation of MAPK and c-Jun may result in an impaired migratory response. It was reported that Foxp3 suppresses both the transcriptional activity and promoter DNA-binding of AP-1 by interacting with c-Jun, and this is related to the unresponsiveness of T_{reg} cells.[11] Our findings suggest that CCR7/$S1P_1$ signaling through the interaction of c-Jun and Foxp3 in T_{reg} cells controls migratory functions, in addition to the unresponsiveness of T_{reg} function. This may explain the defective *in vivo* function of *Ccr7*$^{-/-}$ T_{reg} cells.

S1P is one of the natural lysophospholipids that control various functions of immune cells, such as migration, proliferation, and cytokine secretion.[20–23] S1P is secreted by macrophages, mast cells, dendritic cells, and platelets.[24,25] The concentration of S1P is higher in the blood and lymph (range, 0.1 to 3 μmol/L) than in the lymphoid organs and other tissues (range, 3 to 100 nmol/L).[26,27] The S1P concentration gradient in each organ or tissue can control the chemotactic emigration of thymocytes and egress of lymphocytes from LNs during the differentiation or activation of certain pathological conditions.[28,29] More importantly, the condition of cell surface expression of S1P receptors regulates immune cell functions such as egress from LNs.[30,31] Among the five S1P G protein-coupled receptors (ie, $S1P_1$ though $S1P_5$), $S1P_1$ is the major S1P receptor responsible for the direct chemotactic response in T cells.[32–34] $S1P_1$ expressed on the T-cell surface is internalized when T cells are activated through the binding of S1P-$S1P_1$.[17] In the present study, although total expression of $S1P_1$ in *Ccr7*$^{-/-}$ T_{reg} cells was not significantly changed compared with that in WT T_{reg} cells, migratory function of WT T_{reg} cells in the response to CD3 signaling and S1P was impaired by treatment with a Gi inhibitor. In addition, CCR7 ligand-enhanced migratory response of WT T_{reg} cells was also inhibited by treatment with a Gi inhibitor. This finding suggests that CCR7 controls S1P/$S1P_1$-mediated T_{reg}-specific functions through CD3 signaling. However, the precise mechanism underlying CCR7 and $S1P_1$ signaling remains to be clarified.

TCR/CD3-dependent stimulation of T cells induces the down-regulation of plasma membrane $S1P_1$,[17] and activation of several molecules downstream of $S1P_1$ including Rac-1, ERK, and c-Jun, after AP-1 activation plays a critical role in S1P/$S1P_1$-mediated T cell functions.[15,35] Our results show that the activation of signaling molecules in MAPK and AP-1 pathways through TCR/CD3 and $S1P_1$ in *Ccr7*$^{-/-}$ T_{reg} cells was abrogated. In addition, CD3/S1P-induced transcriptional activity of c-Jun in normal Treg cells was enhanced by the addition of a CCR7 ligand (CCL21 or CCL19). This result suggests that the possible crosstalk between CCR7 and S1P/$S1P_1$ signaling plays an important role in TCR/CD3-mediated activation or peripheral T_{reg} cell migration. A recent report indicates that $S1P_1$ delivers an intrinsic negative signal to restrain thymic generation, peripheral maintenance, and suppressive activity of T_{reg} cells.[36] Furthermore, it was demonstrated that $S1P_1$ induces the selective activation of the Akt-mTOR kinase pathway to impede the development and function of T_{reg} cells.[15] Although the present study was focused on the migratory function of peripheral T_{reg} cells and not the development and function of thymic T_{reg} cells, we note that the Akt-mTOR pathway may be associated with the $S1P_1$-AP-1 pathway. Because the phosphorylation of ERK in *Ccr7*$^{-/-}$ T_{reg} cells was abrogated by stimulation with anti-CD3 mAb and S1P, but ERK activation in WT T_{reg} cells was detectable, it is possible that the Akt-mTOR pathway can act at any step in the $S1P_1$-AP-1 pathway. Our results show that ERK activation through CCR7/CD3/$S1P_1$ signaling is more crucial than Akt-mTOR for the migratory functions of T_{reg} cells. Further analysis of the molecular interactions between various signaling molecules is warranted.

Foxp3 plays an essential role in suppressing AP-1 DNA-binding activity and consequently inhibiting AP-1 transcription activity, because the expression of Foxp3 significantly blocked AP-1 transcriptional activity and promoter DNA binding.[11] A previous report suggested

that the blocking of AP-1 transcriptional activity by Foxp3 is associated with the unresponsiveness of T_{reg} cells because of inhibition of AP-1-mediated activation of T_{reg} cells.[11] In addition, transcriptional activation of c-Jun is inhibited in anergic T cells.[37–39] In the present study, signaling after AP-1 activation of *Ccr7*$^{-/-}$ T_{reg} cells was impaired. As a result, binding of Foxp3 to c-Jun in the nucleus was also undetectable in *Ccr7*$^{-/-}$ T_{reg} cells. The unresponsiveness of T_{reg} cells through the abrogated activation of c-Jun may be related to *in vivo* defects in the function of *Ccr7*$^{-/-}$ T_{reg} cells, as we have previously reported.[14] Mutations within a putative nuclear localization signal near the C-terminal end of the forkhead domain in the Foxp3 gene abrogate nuclear import of the Foxp3 protein.[40] Although the specific abnormality in the Foxp3 gene of *Ccr7*$^{-/-}$ mice is unclear, the impaired signaling of c-Jun by binding Foxp3 in *Ccr7*$^{-/-}$ T_{reg} cells may influence the localization of the Foxp3 protein. However, it is still unclear whether differentiation in the thymus or maturation in the periphery causes abnormal localization of Foxp3 in the nucleus of *Ccr7*$^{-/-}$ T_{reg} cells.

In summary, the present data show that CCR7 signaling can control the migratory response of T_{reg} cells through a possible crosstalk between Foxp3 and the S1P/S1P$_1$-AP-1 pathway. The characterization of this molecular mechanism is important in defining the pathogenesis of autoimmunity based on defects in T_{reg} cellular function.

Acknowledgments

We thank Satoko Katada, Ai Katayama, and Noriko Kino for their technical assistance and Kensuke Takada for the *in vivo* experiments.

References

1. Sakaguchi S: Naturally arising CD4+ regulatory T cells for immunologic self-tolerance and negative control of immune responses. Annu Rev Immunol 2004, 22:531–562
2. Sakaguchi S, Yamaguchi T, Nomura T, Ono M: Regulatory T cells and immune tolerance. Cell 2008, 133:775–787
3. Zheng Y, Rudensky AY: Foxp3 in control of the regulatory T cell lineage. Nat Immunol 2007, 8:457–462
4. Hori S, Nomura T, Sakaguchi S: Control of regulatory T cell development by the transcription factor Foxp3. Science 2003, 299:1057–1061
5. Sakaguchi S, Ono M, Setoguchi R, Yagi H, Hori S, Fehervari Z, Shimizu J, Takahashi T, Nomura T: Foxp3+ CD25+ CD4+ natural regulatory T cells in dominant self-tolerance and autoimmune disease. Immunol Rev 2006, 212:8–27
6. Wan YY, Flavell RA: Regulatory T-cell functions are subverted and converted owing to attenuated Foxp3 expression. Nature 2007, 445: 766–770
7. Zheng Y, Josefowicz SZ, Kas A, Chu TT, Gavin MA, Rudensky AY: Genome-wide analysis of Foxp3 target genes in developing and mature regulatory T cells. Nature 2007, 445:936–940
8. Li B, Saouaf SJ, Samanta A, Shen Y, Hancock WW, Greene MI: Biochemistry and therapeutic implications of mechanisms involved in FOXP3 activity in immune suppression. Curr Opin Immunol 2007, 19:583–588
9. Ono M, Yaguchi H, Ohkura N, Kitabayashi I, Nagamura Y, Nomura T, Miyachi Y, Tsukada T, Sakaguchi S: Foxp3 controls regulatory T-cell function by interacting with AML1/Runx1. Nature 2007, 446: 685–689
10. Wu Y, Borde M, Heissmeyer V, Feuerer M, Lapan AD, Stroud JC, Bates DL, Guo L, Han A, Ziegler SF, Mathis D, Benoist C, Chen L, Rao A: FOXP3 controls regulatory T cell function through cooperation with NFAT. Cell 2006, 126:375–387
11. Lee SM, Gao B, Fang D: FoxP3 maintains Treg unresponsiveness by selectively inhibiting the promoter DNA-binding activity of AP-1. Blood 2008, 111:3599–3606
12. Kurobe H, Liu C, Ueno T, Saito F, Ohigashi I, Seach N, Arakaki R, Hayashi Y, Kitagawa T, Lipp M, Boyd RL, Takahama Y: CCR7-dependent cortex-to-medulla migration of positively selected thymocytes is essential for establishing central tolerance. Immunity 2006, 24:165–177
13. Schneider MA, Meingassner JG, Lipp M, Moore HD, Rot A: CCR7 is required for the in vivo function of CD4+ CD25+ regulatory T cells. J Exp Med 2007, 204:735–745
14. Ishimaru N, Nitta T, Arakaki R, Yamada A, Lipp M, Takahama Y, Hayashi Y: In situ patrolling of regulatory T cells is essential for protecting autoimmune exocrinopathy. PLoS One 2010, 5:e8588
15. Liu G, Burns S, Huang G, Boyd K, Proia RL, Flavell RA, Chi H: The receptor S1P1 overrides regulatory T cell-mediated immune suppression through Akt-mTOR. Nat Immunol 2009, 10:769–777
16. Liao JJ, Huang MC, Graler M, Huang Y, Qiu H, Goetzl EJ: Distinctive T cell-suppressive signals from nuclearized type 1 sphingosine 1-phosphate G protein-coupled receptors. J Biol Chem 2007, 282: 1964–1972
17. Rivera J, Proia RL, Olivera A: The alliance of sphingosine-1-phosphate and its receptors in immunity. Nat Rev Immunol 2008, 8:753–763
18. Means CK, Miyamoto S, Chun J, Brown JH: S1P1 receptor localization confers selectivity for Gi-mediated cAMP and contractile responses. J Biol Chem 2008, 283:11954–11963
19. Matsuyuki H, Maeda Y, Yano K, Sugahara K, Chiba K, Kohno T, Igarashi Y: Involvement of sphingosine 1-phosphate (S1P) receptor type 1 and type 4 in migratory response of mouse T cells toward S1P. Cell Mol Immunol 2006, 3:429–437
20. Goetzl EJ, Rosen H: Regulation of immunity by lysosphingolipids and their G protein-coupled receptors. J Clin Invest 2004, 114: 1531–1537
21. Goetzl EJ, Wang W, McGiffert C, Huang MC, Gräler MH: Sphingosine 1-phosphate and its G protein-coupled receptors constitute a multifunctional immunoregulatory system. J Biol Chem 2004, 92:1104–1114
22. Graeler M, Goetzl EJ: Activation-regulated expression and chemotactic function of sphingosine 1-phosphate receptors in mouse splenic T cells. FASEB J 2002, 16:1874–1878
23. Graeler M, Shankar G, Goetzl EJ: Cutting edge: suppression of T cell chemotaxis by sphingosine 1-phosphate. J Immunol 2002, 169: 4084–4087
24. Olivera A, Rivera J: Sphingolipids and the balancing of immune cell function: lessons from the mast cell. J Immunol 2005, 174: 1153–1158
25. Pappu R, Schwab SR, Cornelissen I, Pereira JP, Regard JB, Xu Y, Camerer E, Zheng YW, Huang Y, Cyster JG, Coughlin SR: Promotion of lymphocyte egress into blood and lymph by distinct sources of sphingosine-1-phosphate. Science 2007, 316:295–298
26. Lee MJ, Van Brocklyn JR, Thangada S, Liu CH, Hand AR, Menzeleev R, Spiegel S, Hla T: Sphingosine-1-phosphate as a ligand for the G protein-coupled receptor EDG-1. Science 1998, 279:1552–1555
27. Schwab SR, Pereira JP, Matloubian M, Xu Y, Huang Y, Cyster JG: Lymphocyte sequestration through S1P lyase inhibition and disruption of S1P gradients. Science 2005, 309:1735–1739
28. Chiba K, Matsuyuki H, Maeda Y, Sugahara K: Role of sphingosine 1-phosphate receptor type 1 in lymphocyte egress from secondary lymphoid tissues and thymus. Cell Mol Immunol 2006, 3:11–19
29. Rosen H, Goetzl EJ: Sphingosine 1-phosphate and its receptors: an autocrine and paracrine network. Nat Rev Immunol 2005, 5:560–570
30. Schwab SR, Cyster JG: Finding a way out: lymphocyte egress from lymphoid organs. Nat Immunol 2007, 8:1295–1301
31. von Wenckstern H, Zimmermann K, Kleuser B: The role of the lysophospholipid sphingosine 1-phosphate in immune cell biology. Arch Immunol Ther Exp (Warsz) 2006, 54:239–251
32. Gräler MH, Huang MC, Watson S, Goetzl EJ: Immunological effects of transgenic constitutive expression of the type 1 sphingosine 1-phosphate receptor by mouse lymphocytes. J Immunol 2005, 174:1997–2003

33. Matloubian M, Lo CG, Cinamon G, Lesneski MJ, Xu Y, Brinkmann V, Allende ML, Proia RL, Cyster JG: Lymphocyte egress from thymus and peripheral lymphoid organs is dependent on S1P receptor 1. Nature 2004, 427:355–360
34. Wang W, Huang MC, Goetzl EJ: Type 1 sphingosine 1–phosphate G protein-coupled receptor (S1P1) mediation of enhanced IL-4 generation by CD4 T cells from S1P1 transgenic mice. J Immunol 2007, 178:4885–4890
35. Windh RT, Lee MJ, Hla T, An S, Barr AJ, Manning DR: Differential coupling of the sphingosine 1-phosphate receptors Edg-1, Edg-3, and H218/Edg-5 to the G(i), G(q), and G(12) families of heterotrimeric G proteins. J Biol Chem 1999, 274:27351–27358
36. Kim CH: Reining in FoxP3(+) regulatory T cells by the sphingosine 1-phosphate-S1P1 axis. Immunol Cell Biol 2009, 87:502–504
37. Kitagawa-Sakakida S, Schwartz RH: Multifactor cis-dominant negative regulation of IL-2 gene expression in anergized T cells. J Immunol 1996, 157:2328–2339
38. Powell JD, Lerner CG, Ewoldt GR, Schwartz RH: The -180 site of the IL-2 promoter is the target of CREB/CREM binding in T cell anergy. J Immunol 1999, 163:6631–6639
39. Sundstedt A, Sigvardsson M, Leanderson T, Hedlund G, Kalland T, Dohlsten M: In vivo anergized CD4+ T cells express perturbed AP-1 and NF-kappa B transcription factors. Proc Natl Acad Sci USA 1996, 93:979–984
40. Lopes JE, Torgerson TR, Schubert LA, Anover SD, Ocheltree EL, Ochs HD, Ziegler SF: Analysis of FOXP3 reveals multiple domains required for its function as a transcriptional repressor. J Immunol 2006, 177:3133–3142

Development, Growth & Differentiation
The Japanese Society of Developmental Biologists

Develop. Growth Differ. (2011) **53**, 48–54 doi: 10.1111/j.1440-169X.2010.01221.x

Original Article

Atelocollagen-mediated systemic administration of myostatin-targeting siRNA improves muscular atrophy in caveolin-3-deficient mice

Emi Kawakami,[1†] Nao Kinouchi,[1†] Taro Adachi,[2] Yutaka Ohsawa,[3] Naozumi Ishimaru,[4] Hideyo Ohuchi,[2] Yoshihide Sunada,[3] Yoshio Hayashi,[4] Eiji Tanaka[1] and Sumihare Noji[2*]

[1]*Department of Orthodontics and Dentofacial Orthopedics, Institute of Health Bioscience, The University of Tokushima Graduate School, 3-18-15 Kuramoto, Tokushima 770-8504;* [2]*Department of Life Systems, Institute of Technology and Science, The University of Tokushima, 2-1 Minami-Jyosanjima-cho, Tokushima 770-8506;* [3]*Department of Neurology, Kawasaki Medical School, 577 Matsushima, Kurashiki City, Okayama 701-0192; and* [4]*Department of Oral Molecular Pathology, Institute of Health Bioscience, The University of Tokushima Graduate School, 3-18-15 Kuramoto, Tokushima 770-8504, Japan*

Small interfering RNA (siRNA)-mediated silencing of gene expression is rapidly becoming a powerful tool for molecular therapy. However, the rapid degradation of siRNAs and their limited duration of activity require efficient delivery methods. Atelocollagen (ATCOL)-mediated administration of siRNAs is a promising approach to disease treatment, including muscular atrophy. Herein, we report that ATCOL-mediated systemic administration of a myostatin-targeting siRNA into a caveolin-3-deficient mouse model of limb-girdle muscular dystrophy 1C (LGMD1C) induced a marked increase in muscle mass and a significant recovery of contractile force. These results provide evidence that ATCOL-mediated systemic administration of siRNAs may be a powerful therapeutic tool for disease treatment, including muscular atrophy.

Key words: atelocollagen, muscle, muscular dystrophy, myostatin, RNA interference.

Introduction

Myostatin (growth differentiation factor 8, GDF8) is a member of the transforming growth factor-β (TGF-β) superfamily of secreted growth factors (McPherron *et al.* 1997). A number of growth factors of this family have been shown to regulate cell growth and differentiation during development. Myostatin is unique among the members of the TGF-β superfamily because its expression is almost exclusively restricted to the skeletal muscle lineage.

Zhu *et al.* (2000) generated transgenic mice that expressed myostatin mutated at its cleavage site under the control of a muscle specific promoter creating a dominant negative myostatin. These mice exhibited a significant (20–35%) increase in muscle mass that resulted from myofiber hypertrophy and not from myofiber hyperplasia. While, mice fully null for myostatin showed muscle masses that were nearly double that of normal muscle and this marked increase in muscle mass was associated with both hypertrophy and hyperplasia (McPherron *et al.* 1997). The difference in muscle mass seen in dominant negative myostatin and null myostatin mice likely results from incomplete dominance of dominant negative myostatin, so that dimerization and cleavage of normal myostatin is not fully blocked in dominant negative myostatin mice. So, lower levels of myostatin inhibition may affect hypertrophy, while higher levels of myostatin inhibition may be required to alter hyperplasia (Zhu *et al.* 2000). Thus, it appears that myostatin specifically downregulates skeletal muscle mass.

Because of its inhibitory role, myostatin downregulation may serve as a potentially important mechanism for treating diseases associated with muscle wasting and degeneration, such as muscular dystrophy. We recently demonstrated that myostatin inhibition induced by overexpression of the myostatin pro-domain prevented

*Author to whom all correspondence should be addressed.
Email: noji@bio.tokushima-u.ac.jp
†These authors contributed equally to this work.
Received 6 August 2010; revised 4 October 2010; accepted 4 October 2010.

muscular atrophy and normalized intracellular myostatin signaling in a mouse model of limb-girdle muscular dystrophy 1C (LGMD1C) (Nishi *et al.* 2002). Furthermore, myostatin inhibition also suppressed muscular atrophy in caveolin-3-deficient mice that expressed a dominant-negative form of the caveolin-3 gene (Ohsawa *et al.* 2006). The dominant negative caveolin-3 mutation was a missense mutation (Pro104Leu) that was expressed under the control of the M-creatine kinase promoter (Sunada *et al.* 2001).

Duchenne muscular dystrophy (DMD) is an X-linked, lethal skeletal muscle disorder caused by mutations in the *dystrophin* gene (Bulfield *et al.* 1984; Yoshimura *et al.* 2007); it is a severe muscle wasting disorder that affects 1/3500 male births (Deconinck & Dan 2007). To date, there is no effective treatment for muscular dystrophy, although gene therapy could be a valuable approach to treating this disease. In a previous study, inhibition of myostatin using anti-myostatin blocking antibodies was employed in an effort to increase muscle mass (Bogdanovich *et al.* 2002). However, the generation of antibodies against recombinant target proteins was a time-consuming, labor-intensive approach.

Recently, RNA interference (RNAi) has emerged as an effective gene silencing method. RNAi refers to sequence-specific, post-transcriptional gene silencing mediated by approximately 22-nucleotide-long small interfering RNAs (siRNAs) generated from longer double-stranded RNAs (dsRNAs) in both plants and animals, ranging from flatworms to humans (Fire *et al.* 1998). RNAi-based approaches have increasingly been developed in which highly specific siRNAs designed to target disease-causing or disease-promoting genes are utilized without the induction of interferon synthesis or non-specific gene suppression (Elbashir *et al.* 2001; de Fougerolles *et al.* 2007). Magee *et al.* (2006) demonstrated that downregulation of myostatin expression via electroporation of a plasmid directing the expression of a short hairpin interfering RNA (shRNA) against myostatin led to a localized increase in skeletal muscle mass. For safety reasons, however, strategies using vector-based delivery systems may be of limited clinical use. Therefore, a more desirable approach would involve the direct application of active siRNAs *in vivo*.

Atelocollagen (ATCOL), a pepsin-treated type I collagen that lacks antigenicity-conferring telopeptides at its N and C termini, has been shown to promote the efficient delivery of chemically unmodified siRNAs to metastatic tumors *in vivo* (Minakuchi *et al.* 2004; Takeshita *et al.* 2005; Takeshita & Ochiya 2006). Based on its practical use as an siRNA delivery platform, we adapted an ATCOL-mediated oligonucleotide system to deliver a myostatin-targeting siRNA into muscle, and found that local or systemic administration of the myostatin-targeting siRNA coupled with ATCOL led to a marked stimulation of muscle growth *in vivo* within a few weeks (Kinouchi *et al.* 2008). In the current study, we examined whether systemic administration of the myostatin-siRNA/ATCOL (Mst-siRNA/ATCOL) complex effectively silenced myostatin expression in LGMD1C mice, and whether it led to increased muscle mass and/or decreased muscle weakness. In the current study, we used the same myostatin-targeting siRNA reported previously (Magee *et al.* 2006), which is predicted to target myostatin mRNA not only in mice, but also in humans, rats, cows, macaques, and baboons.

Materials and methods

Systemic administration of the Mst-siRNA/ATCOL complex to skeletal muscles in LGMD1C mice

The Mst-siRNA and ATCOL complexes were prepared as follows. Equal volumes of siRNA solution (siRNA and 1× siRNA buffer, 40 μmol/L final concentration) and ATCOL (0.05% final concentration) were combined and mixed by vigorous pipetting. For systemic administration, the siRNA/ATCOL complex (200 μL) was introduced intravenously via orbital veins into 20-week-old LGMD1C mice at 0, 4, 7 and 14 days. As a negative control, scrambled siRNAs were injected into 20-week-old LGMD1C mice at 0, 4, 7 and 14 days.

Morphometric analyses

The masseter and quadriceps femoris muscle tissues were dissected 3 weeks after the first Mst-siRNA/ATCOL complex administration. The tissues were snap-frozen in liquid nitrogen-cooled isopentane and sectioned transversely (6 μm) at the center of the masseter and quadriceps femoris muscles using a cryostat (Leica Microsystems). Sections were stained with hematoxylin and eosin (H&E), and fiber sizes were determined by measuring the area of each transversal myofiber within a fixed area. Approximately 100 myofibers were measured for each tissue sample (six to eight fields/tissue section).

Contractile properties of Mst-siRNA/ATCOL complex-treated tibials anterior (TA) muscles

The entire tibials anterior (TA) muscle was removed with its tibial origin intact, and the distal portion of the TA tendon, together with its origin, were secured with a 5-0 silk suture. The TA was then mounted in a vertical tissue chamber and connected to a force transducer, UL-10GR (Minerva, Nagano, Japan), and a length servosystem, MM-3 (Narishige, Tokyo, Japan).

Electrical stimulations were applied using a SEN3301 (Nihon Kohden, Tokyo, Japan) through a pair of platinum wires placed on both sides of the muscle in physiological salt solution (150 mmol/L NaCl, 4 mmol/L KCl, 2 mmol/L $CaCl_2$, 1 mmol/L $MgCl_2$, 5.6 mmol/L glucose, 5 mmol/L Hepes, pH 7.4, and 0.02 mmol/L D-tubocurarine). Muscle fiber length was adjusted incrementally using a micropositioner until peak isometric twitch force responses were obtained (optimal fiber length [L_0]). Maximal tetanic force (P_0) was assessed by stimulation frequencies of 125 pulses/s delivered in 500 ms duration trains with 2 min intervals between each train. After two measurements were taken, the stimulated muscles were weighted after the tendon and bone attachments were removed. All forces were normalized to the physiological cross-sectional area (pCSA), the latter estimated on the basis of the following formula: muscle wet weight (in mg)/(L_0 [in mm] × 1.06 [in mg/mm^3]). The estimated pCSA was used to determine specific tetanic force, and the muscle was quickly frozen in liquid nitrogen-cooled isopentane for morphometric analysis.

Statistical analyses

Error bars indicate standard deviation of the mean. * indicates $P < 0.01$ or $P < 0.05$ in a Student's *t* test.

Results

The Mst-siRNA/ATCOL complex can stabilize and produce a long-term gene silencing effect

In initial experiments to evaluate the persistence and spread of siRNA/ATCOL complexes (100 μL), we injected a BLOCK-iT Alexa Fluor Red Fluorescent Oligo (10 μmol/L) in the masseter muscle of 20-week-old C57BL/6 mice. Mice were killed at 2 weeks, tissue samples were dissected, and Alexa Fluor Red Fluorescent Oligo expression was assessed under conditions identical to those used in myostatin gene transfer experiments. As expected, Alexa Fluor Red Fluorescent Oligo expression was detected near the sites of injection with an uneven distribution pattern across the tissue (Fig. 1, right panel). These observations suggested that the ATCOL and siRNA formed a stable complex capable of producing an efficient, long-term gene silencing effect.

Intravenous administration of myostatin-targeting siRNAs with ATCOL specifically repressed muscle atrophy in LGMD1C mice

Based on our observation that ATCOL formed stable complexes with siRNAs capable of long-term gene silencing, we administered Mst-siRNA/ATCOL or control scrambled siRNA/ATCOL complexes intravenously into 20-week-old LGMD1C mice at 0, 4, 7, and 14 days (Fig. 2A). Strikingly, we observed the enlargement of a number of skeletal muscles, including the lower limbs, masseters, and more in mice treated with Mst-siRNA/ATCOL (Fig. 2B). Since the changes in the lower limb muscles were the most pronounced, we used them for further analyses. Indeed, we also observed a significant increase in muscle fiber size at 3 weeks after the first administration in mice treated with Mst-siRNA/ATCOL (Fig. 2C).

These results indicated that intravenous administration of a myostatin-targeting siRNA with ATCOL specifically induced muscle hypertrophy in LGMD1C mice. The results were expressed as a ratio of the internal control and were analyzed statistically. Mst-siRNA/ATCOL-treated muscles (18.64 ± 4.18 μm) were significantly larger than control muscles (15.49 ± 3.12 μm) ($P < 0.0001$, $n = 100$). Histometric analysis showed that the myofibril sizes of quadriceps muscles treated with the Mst-siRNA/ATCOL complex were significantly larger than those of control quadriceps muscles (Fig. 2C,D). Examination of the sizes of 100 myofibers from each group showed that the Mst-siRNA/ATCOL-treated myofibril population exhibited a shift from smaller to larger sized fibers; the average myofibril size for Mst-siRNA/ATCOL-treated muscle was increased

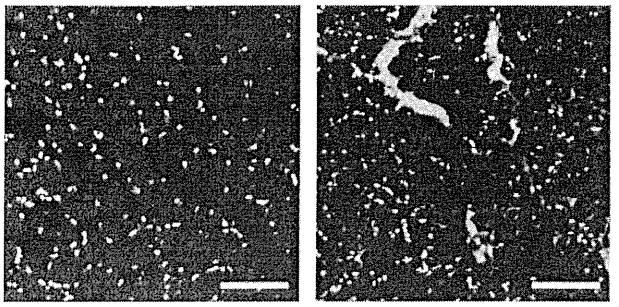

Fig. 1. Persistence and spread of an siRNA/atelocollagen (ATCOL, AteloGene Koken, Tokyo) complex following injection into the masseter muscle. A BLOCK-iT Alexa Fluor Red Fluorescent Oligo (10 μmol/L final concentration, Invitrogen) and ATCOL (100 μL) complex was injected into the masseter muscle of 20-week-old C57BL/6 mice. Gene expression from the BLOCK-iT Alexa Fluor Red Fluorescent Oligo/ATCOL complex injected in masseter muscle was assessed 2 weeks post-injection. Sections were examined following hematoxylin and eosin (H&E) staining (left) and serial section immunofluorescence to detect Alexa Fluor Red-positive cells (right). As expected, the Alexa Fluor Red Fluorescent Oligo expression was not evenly distributed across the tissue, and the majority of expression was located near the injection sites. Images were captured at 400× magnification. Scale bar, 100 μm.

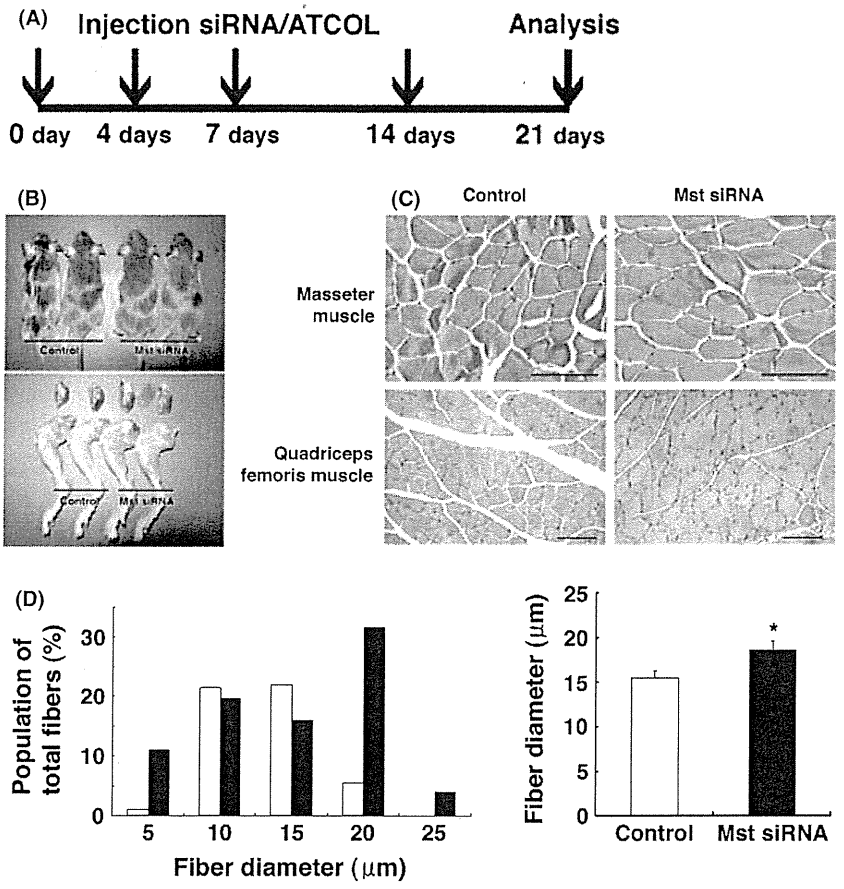

Fig. 2. Systemic administration of the Mst-siRNA/ATCOL complex led to increased skeletal muscle mass and fiber size in LGMD1C mice via inhibition of myostatin expression. In the experiments depicted in (A–C), Mst-siRNA (40 μmol/L final concentration) was mixed with ATCOL according to the manufacturer's instructions. (A) Time course analysis. Twenty-week-old male or female LGMD1C mice were anesthetized with Nembutal (25 mg/kg i.p.), and the Mst-siRNA/ATCOL complex (40 μmol/L in a 200 μL volume) was introduced intravenously via orbital veins at 0, 4, 7, and 14 days (n = 3). As a negative control, scrambled siRNAs were injected into LGMD1C mice. At 3 weeks after the first administration, the quadriceps muscles on both sides were harvested and processed for analysis. (B) Photographs of mice (upper panels) and lower limbs (lower panels). An increase in muscle mass was observed in the Mst-siRNA/ATCOL-treated (right), but not in control mice (left). (C) H&E staining of control (left) and Mst-siRNA/ATCOL-treated (right) masseter or quadriceps femoris muscle. Images of the masseter and quadriceps femoris were captured at 400× and 200×, respectively. Scale bar, 50 μm. (D) Distribution of the myofibril sizes of control (white bars) and Mst-siRNA/ATCOL-treated (black bars) quadriceps muscles. The right panel shows the average myofibril size (15.49 ± 3.12 μm vs. 18.64 ± 4.18 μm, respectively; n = 100; $P < 0.01$). The graphical representation of the data uses the following convention: mean ± SD. Mst-siRNA/ATCOL-treated muscles and mice are shown in black; control muscles and mice are shown in white. National Institute of Health (NIH) Image (NIH) software was used for morphometric measurements.

by approximately 1.2-fold relative to control muscle (Fig. 2D).

Hypertrophied Mst-siRNA/ATCOL-treated LGMD1C muscle fibers exhibit significantly improved contractile force generation

First, we tested the grip strength of mice before and after treatment. There were no statistically significant differences in the grip strength before and after treatment (Fig. 3D). We also evaluated the contractile properties of Mst-siRNA/ATCOL-treated LGMD1C muscle (Fig. 3C). We did not identify any statistically significant differences in the wet weights of Mst-siRNA/ATCOL-treated and untreated LGMD1C muscle. Unexpectedly, the specific force of untreated LGMD1C muscle was much lower than that of Mst-siRNA/ATCOL-treated LGMD1C muscle (Fig. 3A,B). We analyzed the specific force generated by tetanic stimulation (150 Hz) of TA muscles from LGMD1C mice treated with ATCOL-based control scrambled siRNAs or Mst-siRNA (0.568 ± 0.293 vs. 0.041 ± 0.351 N/cm^2, respectively; n = 4; $P < 0.05$).

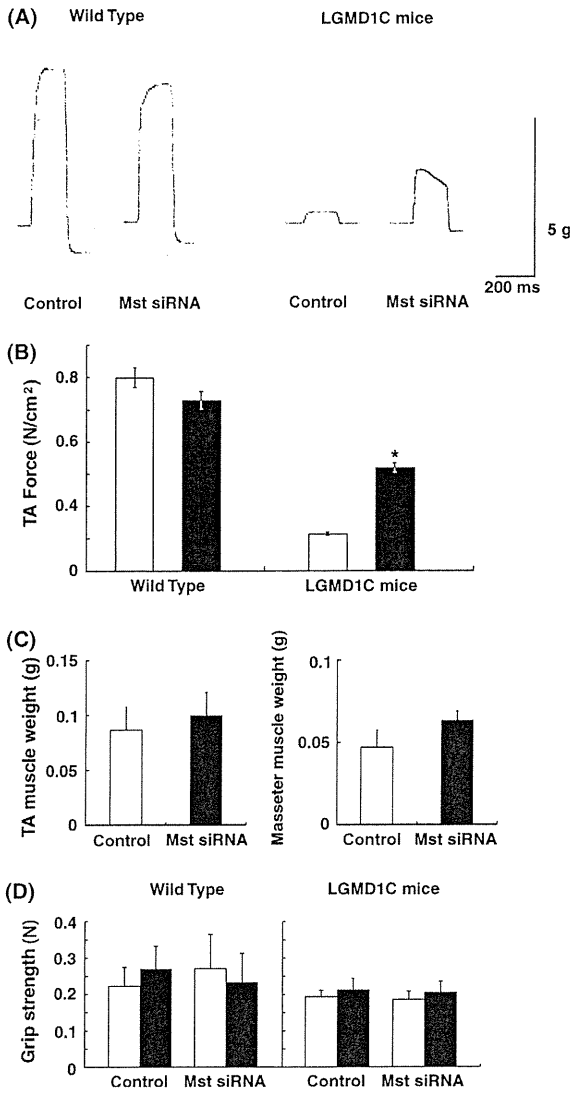

Fig. 3. Mst-siRNA/ATCOL-treated fibers exhibited significantly improved contractile force generation. (A) Specific force generated by tetanic stimulation (150 Hz) of TA muscles from wild-type or LGMD1C mice treated with ATCOL-based control scrambled siRNAs or Mst-siRNA. (B) The specific force of untreated LGMD1C muscle (□) was much lower than that of Mst-siRNA/ATCOL-treated LGMD1C muscle (■) (0.569 ± 0.293 N/cm^2 vs. 0.041 ± 0.351 N/cm^2, respectively; $n = 4$; $P < 0.05$). In contrast, in wild-type mice, the specific force was not different between untreated muscle and Mst-siRNA/ATCOL-treated muscle (0.888 ± 0.588 N/cm^2 vs. 0.925 ± 0.828 N/cm^2; $n = 3$. (C) There were no statistically significant differences in wet weights between untreated muscles and Mst-siRNA/ATCOL-treated muscles. (D) There were no statistically significant differences in grip strength between pre-treated mice (□) and after Mst-siRNA/ATCOL-treated mice (■).

Although wild-type fibers have been found to be hypertrophied (Kinouchi *et al.* 2008), the present results did not show a significant difference between the contractile force generated by Mst-siRNA/ATCOL-treated and untreated wild-type muscle (0.888 ± 0.588 vs. 0.925 ± 0.828 N/cm^2; $n = 3$). As shown in Figure 2D, histogram analysis demonstrated a shift to the right in the fiber distribution of Mst-siRNA/ATCOL-treated LGMD1C muscle relative to that of untreated LGMD1C muscle; larger caliber fibers were dominant, reflecting hypertrophy of Mst-siRNA/ATCOL-treated muscle fibers. Thus, hypertrophied Mst-siRNA/ATCOL-treated LGMD1C muscle fibers exhibited improved contractile force generation, but the increase in muscle weight did not correlate with increased force generation.

We previously reported that local and systemic administration of siRNA against myostatin coupled with ATCOL markedly stimulated muscle growth *in vivo* within a few weeks (Kinouchi *et al.* 2008), and that ATCOL-based gene therapy was associated with low immunogenicity. As expected, we did not observe any signs or symptoms suggestive of health problems during the experimental period of the current study.

Discussion

In the current study, we intravenously administrated a myostatin-targeting siRNA with ATCOL and analyzed the relationship between the extent of Mst-siRNA/ATCOL expression and the recovery of contractile force in LGMD1C muscles. Histogram analysis further demonstrated that the myofibril size distribution of Mst-siRNA/ATCOL-treated LGMD1C muscle fibers was shifted from smaller to larger sized fibers relative to control muscle fibers. We found that treatment of LGMD1C mice with the Mst-siRNA/ATCOL complex led to a significant increase in skeletal muscle mass and enhanced contractile force, similar to that reported previously with a myostatin blockade of dystrophic muscle (Bogdanovich *et al.* 2002).

There was no statistically significant difference in muscle weight between control and Mst-siRNA/ATCOL-treated muscles. It appeared that muscle weight did not correlate with force generation. Thus, hypertrophied Mst-siRNA-positive LGMD1C fibers seemed to greatly improve contractile force generation. Notably, the level of contractile force was dramatically improved by approximately 60% in Mst-siRNA/ATCOL-treated wild-type muscles relative to control muscles. Although the underlying molecular mechanisms by which Mst-siRNA/ATCOL treatment leads to increased contractile force remain to be determined, the current results are encouraging in that the function of caveolin-3-deficient muscles might be greatly improved. These findings are significant because the recovery of absolute maximal force and specific tetanic force are barometers of amelioration (Yoshimura *et al.* 2007).

To our knowledge, the results of the current study are the first to quantitatively and qualitatively demonstrate that *in vivo* myostatin siRNA gene transfer may serve as an effective treatment for muscular dystrophy. The potential benefit of myostatin siRNA gene therapy lies in the treatment of skeletal muscle waste in conditions such as muscular dystrophies (Bogdanovich *et al.* 2002), cachexia and HIV infection in advance of new therapies (Gonzalez-Cadavid & Bhasin 2004; Frimel *et al.* 2005). Although myostatin siRNA gene therapy would not correct the underlying pathophysiology of these diseases, it would counterbalance the effects by stimulating myofiber growth. The ease of administration of the myostatin-siRNA/ATCOL complex combined with its muscle-growth effect makes it a clinically valuable method of fighting against muscle atrophy. However, a strategy for the clinical use of this gene transfer method for human DMD patients requires further testing. Differences between humans and mice, including muscle size, life span and biological properties, should be taken into consideration (Yoshimura *et al.* 2007). In tumor-bearing mice, it was reported that ATCOL distributed siRNAs against luciferase to normal liver, lung, spleen and kidney tissues, as well as to bone-metastatic lesions (Takeshita *et al.* 2005). ATCOL was also reported to display low-toxicity and low-immunogenicity when it is transplanted *in vivo* (Ochiya *et al.* 2001; Sano *et al.* 2003).

Taken together, the results of the present study demonstrate that administration of siRNAs with ATCOL may be a promising therapeutic tool not only for muscular diseases, but also for other genetic diseases. The results of the current study indicate that treatment with Mst-siRNA/ATCOL led to an increase in muscle mass and functional recovery in the absence of obvious adverse effects in LGMD1C mice. The current study also provides evidence of ATOL-mediated delivery of siRNA to skeletal muscle. Therefore, ATCOL-mediated administration of siRNAs represents a powerful new tool for future therapeutic use in the treatment of diseases, including muscular atrophy.

Acknowledgments

We thank Nami Naoe, Masahiro Fujino and Tadashi Okada (Division of Neurology, Kawasaki Medical School) for expert technical assistance. This work was supported by an intramural research grant (20B-13) for neurological and psychiatric disorders of NCNP and a research grant (H20-018) for comprehensive research on disability, health and welfare from the Ministry of Health, Labour and Welfare, a Grant for Research on Psychiatric and Neurological Diseases and Mental Health from the Ministry of Health, Labour and Welfare of Japan (15131301) to Y.O, funding from JSPS KAKENHI (14370212) to YS and Research Project Grants from Kawasaki Medical School (15-115B and 16-601) to Y.O. and Y.S.

References

Bogdanovich, S., Krag, T. O., Barton, E. R., Morris, L. D., Whittemore, L. A., Ahima, R. S. & Khurana, T. S. 2002. Functional improvement of dystrophic muscle by myostatin blockade. *Nature* **420**, 418–421.

Bulfield, G., Siller, W. G., Wight, P. A. & Moore, K. J. 1984. X chromosome-linked muscular dystrophy (mdx) in the mouse. *Proc. Natl Acad. Sci. USA* **81**, 1189–1192.

Deconinck, N. & Dan, B. 2007. Pathophysiology of duchenne muscular dystrophy: current hypotheses. *Pediatr. Neurol.* **36**, 1–7.

de Fougerolles, A., Vornlocher, H. P., Maraganore, J. & Lieberman, J. 2007. Interfering with disease: a progress report on siRNA-based therapeutics. *Nat. Rev. Drug. Discov.* **6**, 443–453.

Elbashir, S. M., Harborth, J., Lendeckel, W., Yalcin, A., Weber, K. & Tuschl, T. 2001. Duplexes of 21-nucleotide RNAs mediate RNA interference in cultured mammalian cells. *Nature* **411**, 494–498.

Fire, A., Xu, S., Montgomery, M. K., Kostas, S. A., Driver, S. E. & Mello, C. C. 1998. Potent and specific genetic interference by double-stranded RNA in Caenorhabditis elegans. *Nature* **391**, 806–811.

Frimel, T. N., Kapadia, F., Gaidosh, G. S., Li, Y., Walter, G. A. & Vandenborne, K. 2005. A model of muscle atrophy using cast immobilization in mice. *Muscle Nerve* **32**, 672–674.

Gonzalez-Cadavid, N. F. & Bhasin, S. 2004. Role of myostatin in metabolism. *Curr. Opin. Clin. Nutr. Metab. Care* **7**, 451–457.

Kinouchi, N., Ohsawa, Y., Ishimaru, N., Ohuchi, H., Sunada, Y., Hayashi, Y., Tanimoto, Y., Moriyama, K. & Noji, S. 2008. Atelocollagen-mediated local and systemic administrations of myostatin-targeting siRNA increase skeletal muscle mass. *Gene Ther.* **15**, 1126–1130.

Magee, T. R., Artaza, J. N., Ferrini, M. G., Vernet, D., Zuniga, F. I., Cantini, L., Reisz-Porszasz, S., Rajfer, J. & Gonzalez-Cadavid, N. F. 2006. Myostatin short interfering hairpin RNA gene transfer increases skeletal muscle mass. *J. Gene Med.* **8**, 1171–1181.

McPherron, A. C., Lawler, A. M. & Lee, S. J. 1997. Regulation of skeletal muscle mass in mice by a new TGF-beta superfamily member. *Nature* **387**, 83–90.

Minakuchi, Y., Takeshita, F., Kosaka, N., Sasaki, H., Yamamoto, Y., Kouno, M., Honma, K., Nagahara, S., Hanai, K., Sano, A., Kato, T., Terada, M. & Ochiya, T. 2004. Atelocollagen-mediated synthetic small interfering RNA delivery for effective gene silencing in vitro and in vivo. *Nucleic Acids Res.* **32**, e109.

Nishi, M., Yasue, A., Nishimatu, S., Nohno, T., Yamaoka, T., Itakura, M., Moriyama, K., Ohuchi, H. & Noji, S. 2002. A missense mutant myostatin causes hyperplasia without hypertrophy in the mouse muscle. *Biochem. Biophys. Res. Commun.* **293**, 247–251.

Ochiya, T., Nagahara, S., Sano, A., Itoh, H. & Terada, M. 2001. Biomaterials for gene delivery: atelocollagen-mediated controlled release of molecular medicines. *Curr. Gene Ther.* **1**, 31–52.

Ohsawa, Y., Hagiwara, H., Nakatani, M., Yasue, A., Moriyama, K., Murakami, T., Tsuchida, K., Noji, S. & Sunada, Y. 2006.

Muscular atrophy of caveolin-3-deficient mice is rescued by myostatin inhibition. *J. Clin. Invest.* **116**, 2924–2934.

Sano, A., Maeda, M., Nagahara, S., Ochiya, T., Honma, K., Itoh, H., Miyata, T. & Fujioka, K. 2003. Atelocollagen for protein and gene delivery. *Adv. Drug Deliv. Rev.* **55**, 1651–1677.

Sunada, Y., Ohi, H., Hase, A., Ohi, H., Hosono, T., Arata, S., Higuchi, S., Matsumura, K. & Shimizu, T. 2001. Transgenic mice expressing mutant caveolin-3 show severe myopathy associated with increased nNOS activity. *Hum. Mol. Genet.* **10**, 173–178.

Takeshita, F., Minakuchi, Y., Nagahara, S., Honma, K., Sasaki, H., Hirai, K., Teratani, T., Namatame, N., Yamamoto, Y., Hanai, K., Kato, T., Sano, A. & Ochiya, T. 2005. Efficient delivery of small interfering RNA to bone-metastatic tumors by using atelocollagen in vivo. *Proc. Natl Acad. Sci. USA* **102**, 12177–12182.

Takeshita, F. & Ochiya, T. 2006. Therapeutic potential of RNA interference against cancer. *Cancer Sci.* **97**, 689–696.

Yoshimura, M., Sakamoto, M., Ikemoto, M., Mochizuki, Y., Yuasa, K., Miyagoe-Suzuki, Y. & Takeda, S. 2007. AAV vector-mediated microdystrophin expression in a relatively small percentage of mdx myofibers improved the mdx phenotype. *Mol. Ther.* **15**, 320–329.

Zhu, X., Hadhazy, M., Wehling, M., Tidball, J. G. & McNally, E. M. 2000. Dominant Negative myostatin produces hypertrophy without hyperplasia in muscle. *FEBS Lett.* **474**, 71–75.

Aire-dependent production of XCL1 mediates medullary accumulation of thymic dendritic cells and contributes to regulatory T cell development

Yu Lei,[1,3] Adiratna Mat Ripen,[1] Naozumi Ishimaru,[2] Izumi Ohigashi,[1] Takashi Nagasawa,[4] Lukas T. Jeker,[5] Michael R. Bösl,[6] Georg A. Holländer,[5] Yoshio Hayashi,[2] Rene de Waal Malefyt,[7] Takeshi Nitta,[1] and Yousuke Takahama[1]

[1]Division of Experimental Immunology, Institute for Genome Research, [2]Department of Oral Molecular Pathology, Institute of Health Biosciences, University of Tokushima, Tokushima 770-8503, Japan
[3]Key Laboratory of Molecular Biology for Infectious Disease of the People's Republic of China Ministry of Education, Institute for Viral Hepatitis, The Second Affiliated Hospital, Chongqing Medical University, Chongqing 400010, China
[4]Department of Immunobiology and Hematology, Institute for Frontier Medical Sciences, Kyoto University, Kyoto 606-8507, Japan
[5]Laboratory of Pediatric Immunology, Center for Biomedicine, University of Basel and The University Children's Hospital of Basel, 4058 Basel, Switzerland
[6]Transgenic Core Facility, Max-Planck-Institute of Biochemistry, 82152 Martinsried, Germany
[7]Merck Research Laboratories, Palo Alto, CA 94304

Dendritic cells (DCs) in the thymus (tDCs) are predominantly accumulated in the medulla and contribute to the establishment of self-tolerance. However, how the medullary accumulation of tDCs is regulated and involved in self-tolerance is unclear. We show that the chemokine receptor XCR1 is expressed by tDCs, whereas medullary thymic epithelial cells (mTECs) express the ligand XCL1. XCL1-deficient mice are defective in the medullary accumulation of tDCs and the thymic generation of naturally occurring regulatory T cells (nT reg cells). Thymocytes from XCL1-deficient mice elicit dacryoadenitis in *nude* mice. mTEC expression of XCL1, tDC medullary accumulation, and nT reg cell generation are diminished in Aire-deficient mice. These results indicate that the XCL1-mediated medullary accumulation of tDCs contributes to nT reg cell development and is regulated by Aire.

CORRESPONDENCE
Yousuke Takahama:
takahama@
genome.tokushima-u.ac.jp

Abbreviations used: cTEC, cortical thymic epithelial cell; CMJ, cortico-medullary junction; mOVA, membrane-bound OVA; mTEC, medullary thymic epithelial cell; *Mtv*, *mammary tumor virus*; nT reg cell, naturally occurring regulatory T cell; RIP, rat insulin promoter; SCZ, subcapsular zone; tDC, thymic DC.

The thymus provides a microenvironment that is central to the establishment of self-tolerance (Takahama, 2006; Anderson et al., 2007; Klein et al., 2009). In the medullary region of the thymus, medullary thymic epithelial cells (mTECs) and thymic DCs (tDCs) display systemic and tissue-restricted self-antigens and cooperate to induce the negative selection of self-reactive thymocytes (Liston et al., 2003; Gallegos and Bevan, 2004; Anderson et al., 2005). mTECs express a diverse set of self-antigens, including the promiscuously expressed tissue-restricted antigens, in part regulated by the nuclear protein Aire (Derbinski et al., 2001; Anderson et al., 2002). tDCs cross-present the mTEC-derived self-antigens (Gallegos and Bevan, 2004), whereas a fraction of tDCs are derived from the circulation importing various self-antigens into the thymus (Bonasio et al., 2006). The cooperation between mTECs and tDCs contributes to the negative selection of tissue-restricted antigen-reactive thymocytes (Gallegos and Bevan, 2004). In addition to the negative selection of self-reactive thymocytes, the thymus produces naturally occurring regulatory T cells (nT reg cells) that are essential for the establishment of self-tolerance (Sakaguchi et al., 2008). It has been suggested that mTECs (Aschenbrenner et al., 2007; Spence and Green, 2008), tDCs (Proietto et al., 2008; Hanabuchi et al., 2010), and their cooperation (Watanabe et al., 2005)

The Rockefeller University Press $30.00
J. Exp. Med. Vol. 208 No. 2 383-394
www.jem.org/cgi/doi/10.1084/jem.20102327